ARMY RESEARCH LABORATORY

Intermolecular Potential for the Hexahydro-1,3,5-trinitro-1,3,5,-s-triazine (RDX) Crystal: A Crystal-Packing, Monte Carlo, and Molecular Dynamics Study

by Dan C. Sorescu, Donald L. Thompson,
and Betsy M. Rice

ARL-TR-1358 May 1997

The findings in this report are not to be construed as an official Department of the Army position unless so designated by other authorized documents.

Citation of manufacturer's or trade names does not constitute an official endorsement or approval of the use thereof.

DESTRUCTION NOTICE—For classified documents, follow the procedures in DOD 5200.22-M. Industrial Security Manual, Section II-19 or DOD 5200.1-R, Information Security Program Regulation, Chapter IX. For unclassified, limited documents, destroy by any method that will prevent disclosure of contents or reconstruction of the document.

Army Research Laboratory
Aberdeen Proving Ground, MD 21005-5066

ARL-TR-1358 **May 1997**

Intermolecular Potential for the Hexahydro-1,3,5-trinitro-1,3,5,-s-triazine (RDX) Crystal: A Crystal-Packing, Monte Carlo, and Molecular Dynamics Study

Dan C. Sorescu, Donald L. Thompson
Oklahoma State University

Betsy M. Rice
Weapons and Materials Research Directorate, ARL

Abstract

We have developed an intermolecular potential that describes the structure of the α-form of the hexahydro-1,3,5-trinitro,1,3,5-s-triazine (RDX) crystal. The potential is composed of pairwise atom-atom (6-exp) Buckingham interactions and charge-charge interactions. The parameters of the Buckingham repulsion-dispersion terms have been determined through a combination of nonlinear least-squares fitting to observed crystal structures and lattice energies and trial-and-error adjustment. Crystal-packing calculations were performed to determine the equilibrium crystallographic structure and lattice energy of the model. There are no significant differences in the geometrical structures and crystal energies resulting from minimization of the lattice energy with and without symmetry constraints. Further testing of the intermolecular potential has been done by performing symmetry-constrained isothermal-isobaric Monte Carlo simulations. The properties of the crystal (lattice dimensions, molecular orientation, and lattice energy) determined from Monte Carlo simulations at temperatures over the range 4.2–300 K indicate good agreement with experimental data. The intermolecular potential was also subjected to isothermal-isobaric molecular dynamics calculations at ambient pressure for temperatures ranging from 4.2 to 325 K. Crystal structures at 300 K are in outstanding agreement with experiment (within 2% of lattice dimensions, and almost no rotational and translational disorder of the molecules in the unit cell). The space-group symmetry was maintained throughout the simulations. Thermal expansion coefficients were determined for the model, and are in reasonable accord with experiment.

ACKNOWLEDGMENTS

This work was supported by the Strategic Environmental Research and Development Program (SERDP), Project PP-695. The work at Oklahoma State University (OSU) was also supported by the U.S. Army Research Office (Grant No. DAAH 04-93-G-0450). Mr. Sorescu wishes to thank Professor John Yates at the University of Pittsburgh for his hospitality during the course of this work. All the authors wish to thank Dr. Cary F. Chabalowski for helpful discussions.

INTENTIONALLY LEFT BLANK.

TABLE OF CONTENTS

INTENTIONALLY LEFT BLANK.

LIST OF FIGURES

LIST OF TABLES

INTENTIONALLY LEFT BLANK.

1. INTRODUCTION

The pursuit of determining the microscopic details of the chemical and physical processes that occur in condensed phase energetic materials has led to the development of a potential energy function to describe the α-form of the hexahydro-1,3,5-trinitro-1,3,5-*s*-triazine (RDX) crystal. Crystalline RDX exists in two phases [1]: the ambient phase (α-solid), for which the structure has been characterized by neutron diffraction measurements [2], and an unstable phase (β-solid), the crystal structure of which has not been determined. RDX is one of the most widely used explosives, and numerous data on the physical and chemical properties exist for this material [3]. However, direct measurements of molecular-level details of the response of RDX to external stimuli (such as heating or shock) are not available. Simulations using models such as that presented here provide invaluable insight into the dynamic responses of the energetic material. This information can be used to determine how to manipulate or control the behavior of the material. Toward this end, we present an atomistic model for the intermolecular interactions in the α-RDX crystal [2]. We will describe the procedure used to develop and parameterize a simple functional form of the intermolecular potential energy in the first part of this paper, and then describe a series of tests to which this model was subjected to determine whether it accurately represents the α-RDX crystal.

Theoretical studies of the past two decades have demonstrated that simple atom-atom pair potentials are sufficient for predicting molecular crystal structures, but the proper development of accurate models is challenging [4]. The main difficulty lies in attaining a proper parameterization of the potential function such that the model reproduces properties of the crystal such as the lattice energy, crystal structure, elastic properties, and phonon frequencies. Often, the resulting potentials can be used to predict properties not included in the original fitting of the function. Also, when large numbers of crystals with similar functional groups are used in the fitting, the potential parameters are transferable [4–6]. Reproduction of properties used in fitting, prediction of properties, and transferability of potential parameters are three metrics used to assess the quality of a model potential.

Numerous studies of organic molecular crystals [4] have demonstrated that in many cases, the intermolecular interactions can be described by using simple isotropic potentials, such as the (6-exp) Buckingham potential

$$V = A\exp(-Br) - C/r^6 \tag{1}$$

or the (6-m) Lennard-Jones potentials

$$V = D/r^m - C/r^6, \tag{2}$$

where m = 8–14.

The repulsion and dispersion parameters A, B, C, and D are assumed to depend only on atom type and thus are transferable. Despite their analytical simplicity, these potentials have accurately described a large class of crystals, particularly nonpolar crystals. A number of sets of such empirical intermolecular potentials for organic crystals containing C, H, N, O, Cl, and S are currently available [4, 6].

A different approach for describing molecular crystals is to consider explicitly the electrostatic interactions between the atoms of the molecules. In the simplest case, the exp 6-1 potentials

$$V = A\exp(-Br) - C/r^6 + E/r, \tag{3}$$

or m-6-1 potentials offer a significant increase in the flexibility and transferability of the nonbonded potential parameters. This form includes the Coulombic interaction between the charges associated with the various atoms in a molecular crystal. As an example, Williams and Starr [7] have shown that the (exp-6-1) potential gives excellent results for calculations of lattice vibrational for aromatic hydrocarbons, and many of the available force fields such as Amber [8],

ECEPP [9], or Dreiding [10] use this type of potential term for simulations of organic, biological, and main-group inorganic crystals.

Despite the success of this kind of representation, many crystals contain substantial anisotropies in the interactions between the molecules in the crystal. Such crystals cannot be adequately described using the simple electrostatic multipoles. Significant progress has been made by the use of the distributed-multipole technique, which has been used to successfully describe hydrogen-bonded structures [11] and π-π interactions [12]. A recently proposed algorithm for relaxation of molecular crystal structures using a distributed multipole electrostatic model provides a promising approach for studying packing of polar crystals [13].

The main objectives of the work presented here were to develop an interaction potential of the α-RDX crystal that both accurately reproduces experimental information and is simple. These objectives must be accomplished since the aim is to use this model in predicting phenomena occurring in condensed-phase RDX, which might be difficult to measure experimentally. If the model is too complex, CPU requirements to calculate bulk properties of the crystal would be prohibitive. If the potential energy function is too simple and cannot reproduce measured data, then the model is not representative of RDX and thus is not useful. We have found that the RDX crystal can be reasonably described using the exp-6-1 potential (equation [3]). Several of the parameters (such as the Coulombic terms) were assigned before the fitting of equation (3) to experimental observables was attempted. The Coulombic terms were determined through fitting of partial charges centered on each atom of the RDX molecule to a quantum mechanically derived electrostatic potential. We also used previously published parameters for H-H and C-C interactions, and assumed traditional combination rules to obtain heteroatom parameters from the homoatom parameters. The remaining parameters were selected such that symmetry-constrained molecular packing calculations reproduced both the crystallographic structure and the lattice energy of the crystal. Throughout all calculations described hereafter, the molecules are assumed to be rigid, and the structure is described by the center-of-mass positions and orientational parameters for each molecule in the unit cell. The intermolecular potential was subjected to additional tests: molecular packing calculations

performed without symmetry constraints, symmetry-restricted isothermal-isobaric Monte Carlo calculations (NPT-MC), and isothermal-isobaric molecular dynamics calculations (NPT-MD).

In section 2, we give details of the analytical form of the intermolecular potential used in the calculations, the accelerated convergence technique employed for evaluation of the lattice sums, and parameterization of the potential function. Section 3 is devoted to analysis of the theoretical methods used for minimization of the lattice energy and the details of the NPT-MC and NPT-MD calculations. Results of crystal-packing, NPT-MC, and NPT-MD calculations are given in section 5. The conclusions drawn from the study are given in section 6.

2. INTERMOLECULAR POTENTIAL

The central problem in classical simulations of molecular crystals is the construction of an analytical potential energy function that accurately represents the intermolecular interactions and thus predicts the structural and thermochemical parameters of the crystal. In this work, we adopt some general principles for atom-atom potentials that have proven to be successful in modeling a large number of organic crystals [4, 14]. In particular, we assume that (1) the intermolecular interactions depend only on the interatomic distances; (2) the interaction potential can be separated in contributions identified as van der Waals and electrostatic; and (3) the same type of van der Waals potential is used for the same type of atoms, independent of their valence state.

We consider the case of a crystal composed of rigid molecules with one molecule in the asymmetric unit. In this case, the maximum number of degrees of freedom is 12 and corresponds to the 6 unit cell constants (l_1, l_2, l_3, α, β, and γ), three rotations (θ_1, θ_2, and θ_3), and 3 translations (τ_1, τ_2, and τ_3) of the rigid molecule. Let N be the number of molecules per unit cell, each molecule of index i having n_i atoms, such that a given atom is identified by indices $i\alpha$. The position of each unit cell in the bulk is given by $\mathbf{n}=n_1\mathbf{l}_1+n_2\mathbf{l}_2+n_3\mathbf{l}_3$, where n_1, n_2, and n_3 are any combination of integers and $\mathbf{l}_i$ (i=1,2,3) are the vectors defining the edges of the unit cell. The reciprocal space vectors $\mathbf{k}_m$ are defined using the matrix of basis vectors $\vec{\mathbf{h}}=[\mathbf{l}_1,\mathbf{l}_2,\mathbf{l}_3]$

$$\mathbf{k}_m = (\overleftrightarrow{\mathbf{h}}^{-1})^t \begin{pmatrix} m_1 \\ m_2 \\ m_3 \end{pmatrix}, \tag{4}$$

with m_1, m_2, m_3 integers.

In the present treatment we approximate the intermolecular lattice energy of the crystal as a pairwise sum of Buckingham (repulsion and dispersion) and Coulomb potentials of the form

$$E = E_{rep} - E_{disp} + E_{Coul}, \tag{5}$$

with

$$E_{rep} = \frac{1}{2}\sum_{\mathbf{n}}^{\infty *}\sum_{i=1}^{N}\sum_{\alpha=1}^{n_i}\sum_{j=1}^{N}\sum_{\beta=1}^{n_j} A_{i\alpha j\beta}\exp(-B_{i\alpha j\beta}\, r_{ni\alpha j\beta}), \tag{6}$$

$$E_{disp} = \frac{1}{2}\sum_{\mathbf{n}}^{\infty *}\sum_{i=1}^{N}\sum_{\alpha=1}^{n_i}\sum_{j=1}^{N}\sum_{\beta=1}^{n_j} C_{i\alpha j\beta} / r_{ni\alpha j\beta}^{6}, \tag{7}$$

and

$$E_{Coul} = \frac{1}{2}\sum_{\mathbf{n}}^{\infty *}\sum_{i=1}^{N}\sum_{\alpha=1}^{n_i}\sum_{j=1}^{N}\sum_{\beta=1}^{n_j} q_{i\alpha} q_{j\beta} / r_{ni\alpha j\beta}, \tag{8}$$

where $r_{ni\alpha j\beta}=|\mathbf{r}_{i\alpha}-\mathbf{r}_{j\beta}+\mathbf{n}|$ is the distance between atom α of molecule i and atom β of molecule j, located in the cell determined by the set (n_1,n_2,n_3). The summation $\sum_{\mathbf{n}}^{\infty *}$ in equations (6)–(8) excludes the terms with i=j, when $|\mathbf{n}|=0$.

In performing these lattice sums, special attention should be paid to the dispersion and Coulombic sums (equations [7] and [8], respectively) due to their slow convergence over the infinite periodic lattice. For the treatment of these terms, we adopt the method of accelerated convergence of the crystal-lattice potential sums introduced by Williams [15, 16]. In this procedure, a general lattice sum S_m of the form

$$S_m = \frac{1}{2}\sum_{\mathbf{n}}^{\infty *}\sum_{i=1}^{N}\sum_{\alpha=1}^{n_i}\sum_{j=1}^{N}\sum_{\beta=1}^{n_j} \lambda_{i\alpha}\lambda_{j\beta} / r_{ni\alpha j\beta}^{m}, \tag{9}$$

is transformed by multiplying the terms of the series by a convergence function $\Phi_m(r)$:

$$S_m = \frac{1}{2}\sum_{\mathbf{n}}^{\infty *}\sum_{i=1}^{N}\sum_{\alpha=1}^{n_i}\sum_{j=1}^{N}\sum_{\beta=1}^{n_j} \lambda_{i\alpha}\lambda_{j\beta}\Phi_m(r_{ni\alpha j\beta}) / r_{ni\alpha j\beta}^{m}$$

$$+ \frac{1}{2}\sum_{\mathbf{n}}^{\infty *}\sum_{i=1}^{N}\sum_{\alpha=1}^{n_i}\sum_{j=1}^{N}\sum_{\beta=1}^{n_j} \lambda_{i\alpha}\lambda_{j\beta}[1-\Phi_m(r_{ni\alpha j\beta})] / r_{ni\alpha j\beta}^{m}. \tag{10}$$

The function $\Phi_m(r)$ rapidly decreases to zero with increasing r and $\Phi_m(0)=1$.

As a result of this transformation, the first term in equation (10) converges much faster than the original sum S_m in equation (9) and can be evaluated in the real space. The second term in equation (10) is still a slowly varying function of r, but can be determined at a much higher convergence rate when it is Fourier transformed and evaluated in the reciprocal lattice vector space. The convergence function $\Phi_m(r)$ is chosen to be the normalized incomplete gamma function

$$\Phi_m(r) = \frac{1}{\Gamma(m/2)}\int_{\eta^2 r^2}^{\infty} t^{m/2-1}e^{-t}dt \tag{11}$$

of index m=1 for the electrostatic case and m=6 for the dispersion sums. The adjustable parameter η in equation (11) has the dimension of inverse length and determines the relative contributions of the real- and reciprocal-space terms. The contribution of reciprocal-space series increases as η increases. Details of the numerical manipulations can be found in Williams [15, 16], Nijboer and Dewette [17], and Karasawa and Goddard [18].

Under the assumption of neutrality for the total electrostatic charge of each molecule, the expression of the Coulombic energy determined using the accelerated convergence method can be written as superposition of a summation evaluated in the real space, E^1_{dir}, one evaluated in the reciprocal space, E^1_{rec}, plus a set of correction terms, E^1_{cor}, that correspond to exclusion of the self-energy and subtraction of intramolecular interactions:

$$E_{Coul} = E^1_{dir} + E^1_{rec} + E^1_{cor}. \tag{12}$$

The analytic expressions of these sums are:

$$E^1_{dir} = \frac{1}{2}\sum_{\mathbf{n}}^{\infty} {}^{*} \sum_{i=1}^{N} \sum_{\alpha=1}^{n_i} \sum_{j=1}^{N} \sum_{\beta=1}^{n_j} \frac{q_{i\alpha} q_{j\beta}}{r_{ni\alpha j\beta}} \operatorname{erfc}(a_1), \tag{13}$$

$$E^1_{rec} = \frac{1}{2\pi V} \sum_{\mathbf{k}_m \neq 0} |S_1(\mathbf{k}_m)|^2 \frac{\exp(-b_1^2)}{k_m^2}, \tag{14}$$

and

$$E^1_{cor} = -\frac{\eta_1}{\sqrt{\pi}} \left(\sum_{i=1}^{N} \sum_{\alpha=1}^{n_i} q_{i\alpha}^2 \right) - \frac{1}{2} \sum_{i=1}^{N} \sum_{\alpha=1}^{n_i - 1} \sum_{\beta=\alpha+1}^{n_i} \frac{q_{i\alpha} q_{i\beta}}{r_{i\alpha i\beta}} \operatorname{erf}(a_1). \tag{15}$$

In equations (13) and (15), erfc(...) and erf(...) are the complementary error and error functions, respectively. In equation (14) $V=\mathbf{l}_1(\mathbf{l}_2 \times \mathbf{l}_3)$ is the volume of the unit cell. The parameters in equations (13) and (14) are defined as $a_1=\eta_1 r_{ni\alpha j\beta}$ and $b_1=\pi k_m/\eta_1$. The term $S_1(\mathbf{k}_m)$ denotes the structure factor defined as

$$S_1(\mathbf{k}_m) = \sum_{i=1}^{N} \sum_{\alpha=1}^{n_i} q_{i\alpha} \exp(-2\pi i \mathbf{k}_m \mathbf{r}_{i\alpha}). \tag{16}$$

Similarly, application of the accelerated convergence technique to the case of the dispersion energy yields the following summations [16]:

$$E^6_{dir} = \frac{1}{2}\sum_{\mathbf{n}}^{\infty} * \sum_{i=1}^{N}\sum_{\alpha=1}^{n_i}\sum_{j=1}^{N}\sum_{\beta=1}^{n_j} \frac{C_{i\alpha j\beta}}{r^6_{ni\alpha j\beta}} (1 + a_6^2 + a_6^4/2)\exp(-a_6^2), \tag{17}$$

$$E^6_{rec} = \frac{\pi^{9/2}}{3V}\sum_{\mathbf{k}_m\neq 0} |S_6(\mathbf{k}_m)|^2 k_m^3 \left[\sqrt{\pi}\,\mathrm{erfc}(b_6) + \left(\frac{1}{2b_6^3} - \frac{1}{b_6}\right)\right]\exp(-b_6^2), \tag{18}$$

and

$$E^6_{cor} = \frac{\pi^{3/2}\eta_6^3}{6V}\left(\sum_{i=1}^{N}\sum_{\alpha=1}^{n_i} C_{i\alpha i\alpha}^{1/2}\right)^2 - \frac{\eta_6^6}{12}\left(\sum_{i=1}^{N}\sum_{\alpha=1}^{n_i} C_{i\alpha i\alpha}\right)$$

$$-\frac{1}{2}\sum_{i=1}^{N}\sum_{\alpha=1}^{n_{i-1}}\sum_{\beta=\alpha+1}^{n_i}\left[2-(2 + 2a_6^2 + a_6^4)\exp(-a_6^2)\right]\frac{C_{i\alpha i\beta}}{r_{i\alpha i\beta}}. \tag{19}$$

The first term in equation (17) represents the contribution in the limit $\mathbf{k}_m \to 0$ of the Fourier transform of the second term in equation (10). The second term in equation (19) is the self-energy, and the last term of equation (19) represents the contribution of intermolecular dispersion terms. The definitions of parameters a_6 and b_6 are similar to those previously given for a_1 and b_1, but correspond to a different adjustable parameter, η_6. Similarly, the definition of $S_6(\mathbf{k}_m)$ is that of equation (16), but with charges $q_{i\alpha}$ replaced by potential terms $(C_{i\alpha})^{1/2}$.

For rigid molecules (which are assumed in this study), the terms corresponding to self-energies and intramolecular energies do not contribute to the derivatives of the lattice energy. In the case when the molecules in the unit cell are related by symmetry, the general expressions

equations (13)–(15) and equations (17)–(19) representing the energy of a unit cell can be further reduced. Full details of this particular case are given in Williams [16].

In practice, the interactions in real space are calculated for atom pairs separated by no more than a given cutoff distance (r_{cut}). Interactions between atom pairs separated by distances larger than r_{cut} are assumed to be zero. Once r_{cut} is specified, the parameters η_1 and η_6 are then chosen to ensure the proper convergence of the lattice sums in both real and reciprocal space while limiting the computational expense of the calculations of the sums [18, 19].

An optimal set of potential parameters can be obtained by minimizing a general function of the form

$$R = \sum_{i,j} w_{ij}\left(\frac{\partial E}{\partial p_i}\right)\left(\frac{\partial E}{\partial p_j}\right) + w'\left(E-E^0\right)^2 \qquad (20)$$

at the observed equilibrium structure. The function R in equation (20) represents a weighted superposition of forces and torques plus the square of the difference between the calculated lattice energy E and the measured value E^0 [20]. The weight elements w_{ij} are calculated as $\left[\tilde{\mathbf{H}}^t \mathbf{V} \tilde{\mathbf{H}}\right]^{-1}_{ij}$, where $\left[\tilde{\mathbf{H}}\right]$ is the Hessian matrix ($H_{ij}=\partial^2 E/\partial p_i \partial p_j$) and $\mathbf{V}$ is a diagonal matrix with elements $V_{ii}=\sigma^2(p_i)$, equal to the allowed error threshold of different structural parameters. The static lattice energy E^0 in equation (20) can be estimated from the experimental enthalpy of sublimation by using the relation [21]: $-\Delta H_0^{subl} = E+K_0+2RT$, where E is the lattice energy and K_0 is the zero-point energy. We have made the approximation that the static lattice energy is equal to the measured sublimation enthalpy of the RDX crystal (−130.1 kJ/mole) [22]. Discussions of alternative techniques used for optimization of potential parameters can be found in Hsu and Williams [20].

Several of the potential parameters, including all of the electrostatic charges, were assigned before optimization of equation (20) was attempted. The assignment of the electrostatic charges

poses a problem in that the atom-centered monopole charge is not an observable quantity and cannot be obtained directly from either experiment or first principles calculations. There are several schemes for evaluation of charges by empirical partition or by using a quantum mechanically derived wave function [23]. We have chosen to make the assignments for the atom-centered monopole charges by using the set that best reproduces the quantum mechanically derived electrostatic potential that is calculated over grid points surrounding the van der Waals surface of the RDX molecule. This method of fitting to the electrostatic potential was proposed by Breneman and Wiberg [24], and is incorporated in the Gaussian 94 package of programs [25] under the keyword CHELPG. This method presents the advantages of having a higher density of points and a better selection procedure, which ensures a decrease of rotational variables observed with similar methods. The electronic structure calculations were performed at the MP2/6-31G** level [26–28]. The atomic arrangement of the molecule used in these calculations was consistent with the crystallographic configuration [2]. A total number of 11,900 points were used in the fit, leading to a root-mean-square deviation of 0.00259. The resulting electrostatic charges are given in Table 1.

The number of parameters to be fit was further reduced by using traditional combination rules to obtain the heteroatom parameters from homoatom parameters:

$$A_{\alpha\beta} = \sqrt{A_{\alpha\alpha}A_{\beta\beta}},$$

$$B_{\alpha\beta} = (B_{\alpha\alpha} + B_{\beta\beta})/2,$$

$$C_{\alpha\beta} = \sqrt{C_{\alpha\alpha}C_{\beta\beta}}. \qquad (21)$$

We have used the published 6-exp parameters [29] for the H-H and C-C nonbonded interactions and have optimized the values of N-N and O-O interactions. It has been shown that there is a strong correlation between the nonbonded potential parameters A and B [28].

Thus, we have used published values [27] for B parameters for the N-N and O-O interactions and optimized the corresponding A and C parameters.

Table 1. Electrostatic Charges for an RDX Molecule

Atom[a]	Charge/|e|
C_1	-0.092940
C_2	-0.015018
C_3	-0.045006
N_1	0.038600
N_2	-0.331673
N_3	-0.340479
N_4	0.557379
N_5	0.781316
N_6	0.772447
O_1	-0.356222
O_2	-0.366350
O_3	-0.369139
O_4	-0.380884
O_5	-0.358609
O_6	-0.378756
H_1	0.130328
H_2	0.174188
H_3	0.161566
H_4	0.146993
H_5	0.113532
H_6	0.158728

[a] The atom indices are consistent with the labels in Figure 2.

After making these assignments, a two-step calculation was performed iteratively until a suitable parameter set was obtained. The first step in the iteration involved selection of a trial parameter set through a combination of trial-and-error adjustments of parameters and minimization of equation (20). The model using the trial parameter set was then subjected to symmetry-constrained molecular packing calculations using the PCK91 set of programs [29] (described in the next section). These two steps were repeated until a parameter set that reproduced experimental information to the desired tolerance was obtained. The PCK91 set of programs allows analytical derivatives of the potential only in the direct space. To circumvent the problem arising from the inability of the PCK91 programs [29] to evaluate the derivatives of the reciprocal space terms (equations [14] and [18]), we set the cutoff distance in the real space to 17.0 Å. By choosing such a large cutoff, we were able to adjust the parameters η_1 and η_6 such that the reciprocal sums are smaller than the desired errors in the evaluation of equation (20). Thus, evaluation of the reciprocal terms using these parameters became unnecessary. The values obtained for η_1=0.1861 and η_6=0.2304 assured contributions of the reciprocal sums smaller than 0.01 kJ/mol. This large cutoff was also used in the subsequent full-minimization-molecular packing and symmetry-constrained Monte Carlo calculations described as follows.

The quality of the fit was judged according to two discrepancy factors. The first is a structural shift factor of the form

$$F_1 = (50\Delta\theta)^2 + (10\Delta x)^2 + \sum_{j=1}^{3}\left(100\frac{\Delta l_i}{l_i}\right)^2 + \sum_{j=1}^{3}(\Delta\alpha_i)^2, \qquad (22)$$

where $\Delta\theta$ is the total rms rigid-body rotational displacement (in radians) after minimization, Δx the rms total rigid-body translational displacement (in Å), l_i the lengths of the edges of the unit cell, and α_i the angles of the unit cell. The second discrepancy factor, F_2, was calculated from F_1 by including the weighted difference between the calculated lattice energy and the observed lattice energy. The threshold values are those previously proposed by Starr and Williams [31]:

unit-cell edge of 1%, cell angles and molecular rotations at 0.02 rad, molecular translations of 0.05 Å, and heats of sublimation of 0.02 kJ/mol.

A (3×3×3) block of unit cells of RDX with each unit cell identical to the structure determined by single-crystal neutron diffraction experiments [2] was used in the parameterization of the potential energy function. The refined structure of RDX at room temperature, 1 atm, belongs to the orthorhombic space group Pbca with Z=8 molecules per unit cell (see Figure 1). The cell parameters are l_1=13.182 Å, l_2=11.574 Å, and l_3=10.709 Å, giving the volume of the unit cell as 1633.8557 Å^3. As shown in Figure 2, the molecule consists of three alternating N-NO_2 and CH_2 groups arranged in a six-membered C-N puckered ring.

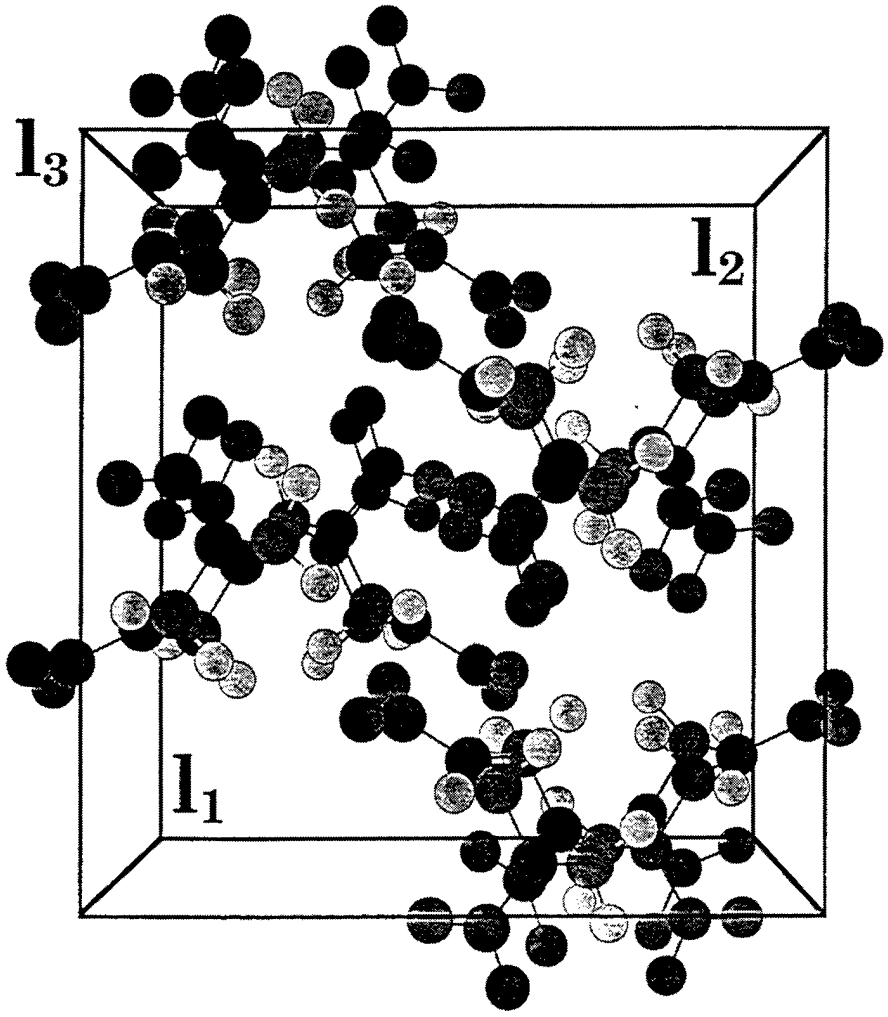

Figure 1. Unit cell of α-RDX crystal using refined coordinates given in Choi and Prince [2].

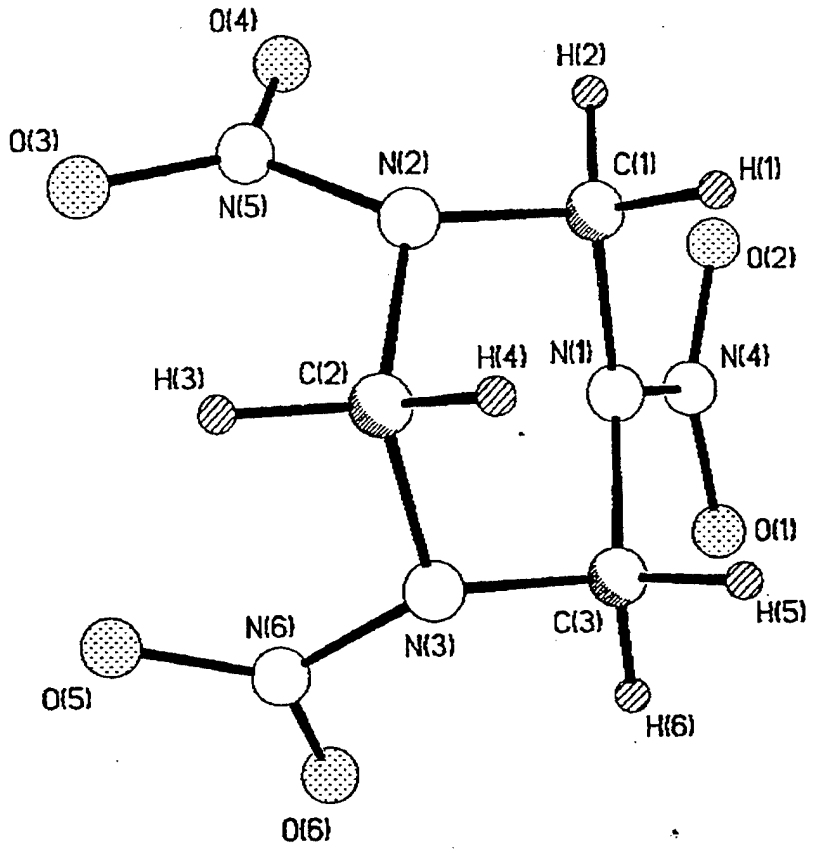

Figure 2. Molecular configuration of an RDX molecule.

The values of the complete set of optimized intermolecular parameters are given in Table 2, and the values of the crystal parameters resulting from the symmetry-constrained energy minimization using these parameters are given in Table 3. A total translation of 0.126 Å and a total rotation of 1.241° away from the experimental values for the molecule in the asymmetric unit take place in the minimization process. The corresponding values of the discrepancy factors are F_1=0.88 and F_2=0.57.

3. DETAILS OF THE CALCULATIONS

Three series of calculations—molecular packing, symmetry-constrained isothermal-isobaric Monte Carlo, and isothermal-isobaric molecular dynamics calculations—were performed to

Table 2. RDX Atom-Atom Potential Parameters

Pair (α–β)	$C_{\alpha\beta}$ (kJ/mol Å^6)	$B_{\alpha\beta}$ (Å^{-1})	$A_{\alpha-\beta}$ (kJ/mol)
H-H	136.3800	3.74	9213.510
C-C	2439.3459	3.60	369726.330
N-N	1668.3316	3.78	264795.246
O-O	1453.3114	3.96	290437.820

assess the quality of the potential energy function. Details of the methods for each of the calculations are described herein. In each of the calculations, the set of refined coordinates from the neutron-diffraction study [2] was used for the initial geometry of the system.

3.1 Molecular Packing. Molecular packing calculations are minimizations of the lattice energy with respect to structural degrees of freedom of the crystal. For the particular case of crystals with one molecule in the asymmetric unit occupying an arbitrary position, the maximum number of structural degrees of freedom is 12. A reduced number of structural degrees of freedom might be involved, depending on the symmetry restrictions of different space groups.

Assuming that the crystal energy is known as a function of the structural lattice parameters, the equilibrium crystal configuration is determined by the conditions of zero force and torques, together with the requirement that there is a minimum. The search for such a minimum can be done using a combination of steepest-descent and Newton-Raphson procedures [15, 32].

The Newton-Raphson method is used to minimize the lattice energy for configurations close to the equilibrium, when all eigenvalues of the Hessian matrix are positive definite. In this case, the step for the iterative search for a minimum energy from a trial configuration is determined as

$$\Delta \mathbf{p} = -[\tilde{\mathbf{H}}(\mathbf{p})]^{-1}\,\mathbf{G}(\mathbf{p}), \tag{23}$$

Table 3. Lattice Parameters and Energy Obtained in Crystal-Packing Calculations With (PCK91) and Without (LMIN) Symmetry Constraints

Method	Q[a]	Final Energy[b]		Final Lattice Parameters[c]					
		NB	ES	1_1	1_2	1_3	α	β	γ
PCK91		-85.0061	-45.0834	13.2862	11.6511	10.6081	90.000[d]	90.000[d]	90.000[d]
LMIN	5.5	-83.9420	-45.0475	13.2883	11.6532	10.6109	90.001	90.000	89.998
	7.5	-84.5993	-45.0684	13.2870	11.6518	10.6095	90.000	90.002	89.999
	10.5	-84.8646	-45.0767	13.2866	11.6513	10.6088	90.001	90.003	90.002
	20.5	-84.9891	-45.0807	13.2863	11.6510	10.6086	90.001	90.003	90.000
	30.5	-84.99965	-45.0811	13.2863	11.609	10.6085	90.001	90.002	90.001
	40.5	-85.0048	-45.0813	13.2863	11.6509	10.6086	90.000	90.002	90.000
Expt.[e]				13.182	11.574	10.709	90.00	90.00	90.00

[a] Value of the cutoff parameter as described in text.
[b] Nonbonded (NB) and electrostatic (ES) energies per molecule in kJ/mol.
[c] Lattice dimensions 1_1, 1_2, and 1_3, in Å and angles α , β and γ in degrees.
[d] Fixed throughout minimization.
[e] Reference [2].

where $\mathbf{G}$ is the vector of first derivatives and $\tilde{\mathbf{H}}$ is the matrix of second derivatives of the lattice energy with respect to the structural variables. This procedure is repeated until no significant changes are observed in the coordinates, and the first derivatives of the energy are close to zero.

In those situations when the Hessian is not positive definite for the trial configuration, the steepest-descent method is used. In this procedure, the searching step is taken along the direction of the local downhill gradient [32]. This method has a low rate of convergence near the minimum, but can be efficiently used to determine a configuration for which the Newton-Raphson method can be used.

The molecular packing program PCK91 [29] was used in the determination of a suitable parameter set. This program was used to find energy minima for systems described by the trial parameter sets. This program calculates crystal lattice sums using the accelerated convergence method in section 2, and the first and second derivatives of the crystal lattice energy are evaluated analytically. The space group symmetry is maintained throughout the energy minimization. This reduces the number of independent variables in the minimization procedure, resulting in a significant decrease of computational time when compared to a nonconstrained energy minimization. The crystallographic parameters varied in the minimization using PCK91 [29] are the three dimensions of the unit cell and the three respective translations and rotations of a central molecule (from which the positions of all other molecules in the unit cell can be determined through symmetry operations). The angles of the unit cell were frozen at 90°.

A necessary condition in assessing the accuracy of the empirical potential energy is that the structure corresponding to the energy minimum of the model should maintain the observed space group symmetry [34]. In order to test our potential for such a requirement, we have used an algorithm recently proposed by Gibson and Scherega [35] for efficient minimization of the energy of a fully variable lattice composed by rigid molecules. This algorithm makes use of Gay's [36] secant-type unconstrained minimization solver (SUMSL) routine to minimize the lattice energy. The gradients of the energy with respect to generalized coordinates (i.e., 6Z rigid-body parameters of the Z molecules in the unit cell and the six lattice parameters) are evaluated

analytically. The nonbonded interactions were cut off at a distance Qσ with a cubic feather (spline) applied over the distance Pσ-Qσ to ensure that the energy and its first derivatives are continuous everywhere. Here, the P and Q parameters specify, respectively, the start and the end of the feather, and σ is the value of interatomic potential at which $E = 0$ and $dE/dr < 0$. Long-range Coulombic interactions are evaluated based on an Ewald type of transformation.

At the beginning and at the end of lattice energy minimization, the symmetry operations that transform the molecules in the unit cell are computed, and if these operations remain unchanged, the space group is considered conserved; otherwise, a new space group is deduced based on the final symmetry relations. Some of the symmetry transformations can be lost during energy minimization but are regained before convergence takes place [34].

We have used the algorithm as implemented in the program LMIN [37] to analyze the accuracy of the proposed intermolecular potential for the RDX crystal. In all of these calculations, the parameter P was set equal to ~Q–5.

3.2 Symmetry-Constrained NPT Monte Carlo Calculations. The intermolecular potential was further evaluated based on its performance in Monte Carlo calculations in the NPT ensemble [19]. These calculations were used to determine some of the crystal parameters as functions of temperature and pressure as predicted by the model. In these calculations, we have constrained the crystal symmetry as in the first series of molecular packing calculations using PCK91 [29]. The simulation box contains all unit cells from −3,3 along the $\mathbf{l}_1$ axis, −3,4 along the $\mathbf{l}_2$ axis, and −3,4 along the $\mathbf{l}_3$ axis, with the central cell occupying position (0,0,0). The positions of the molecules inside the unit cell, considered as rigid entities, are determined from the coordinates of a single molecule in the unit cell, which is denoted hereafter as (T). The coordinates of all remaining molecules in the crystal of RDX are obtained from the fractional positions of (T) by applying the operators of the crystal space group Pbca [38]. The position of (T) inside the unit cell is described by a set of fractional coordinates of the mass center, and the molecular orientation is described by a set of quaternions [19, 39]. Because of the symmetry constraints within the simulation, each molecule in this system has the same number and spatial arrangement

of neighbors as (T) at each step in the NPT-MC simulation. Using these symmetry constraints, the total potential energy of a system,

$$E = \frac{1}{2} \sum_{n}^{\infty} * \sum_{i=1}^{N} \sum_{\alpha=1}^{n_i} \sum_{j=1}^{N} \sum_{\beta=1}^{n_j} E_{i\alpha j\beta}, \tag{24}$$

can be written in terms of the potential energy of a single molecule (T),

$$E = \frac{N}{2} \sum_{n}^{\infty} * \sum_{\alpha=1}^{n_T} \sum_{j=1}^{N} \sum_{\beta=1}^{n_j} E_{T\alpha j\beta}. \tag{25}$$

Therefore, in this type of simulation, it is necessary to calculate only the potential energy for the single molecule (T) (equation [25]) rather than perform the summations over all molecules as given in equation (24). The computational demands of symmetry-constrained NPT-MC simulations are much less than nonconstrained NPT-MC simulations, since the phase space that is sampled is reduced to the structural parameters corresponding to a single molecule. We found in this and a previous study [40] that the simulations provide averages that do not differ radically from non-symmetry-constrained NPT-MC predictions. This allows for rapid testing of intermolecular interaction potentials using the method of Monte Carlo. Poor potentials can be eliminated quickly with these inexpensive calculations, while potentials that show reasonably good results in these simulations can be subjected to more rigorous nonconstrained simulations such as those described later.

The general method followed in performing the MC-NPT calculations is that described in Allen and Tildesley [19]. Here we will discuss only the main steps of this procedure. The sampling in the MC walk was performed over the three cell constants corresponding to unit cell edges, the fractional coordinates of the mass-center, and the set of quaternions of (T). The angles of the unit cell were frozen at 90°. At every step during the Markov walk, a trial to randomly

modify both the position and orientation of (T) and one edge of the unit cell was attempted. These types of displacements were performed according to the relations:

$$s_i^{new} = s_i^{old} + (2\xi_1 - 1)\Delta s_{max}, \quad i=x,y,z$$

$$q_i^{new} = q_i^{old} + (2\xi_2 - 1)\Delta q_{max}, \quad i=1,2,3,4$$

$$l_i^{new} = l_i^{old} + (2\xi_3 - 1)\Delta l_{max}, \quad i=1,2,3, \tag{26}$$

where ξ_1, ξ_2, and ξ_3 are random numbers uniformly distributed in the interval (0,1), and Δs_{max}, Δq_{max}, and Δl_{max} are the maximum allowed changes of the fractional coordinates of the mass center, quaternions, and unit cell dimensions, respectively. The maximum displacements are continuously adjusted using the procedure described in Allen and Tildesley [19] to maintain an acceptance/rejection ratio of about 50%.

After each trial move, the new coordinates of the molecules in the crystal, the new volume V, and the new interaction energy E_{new} (equation [25]) were calculated. The acceptance or rejection of each trial move was decided according to the probability min(1,exp[$-\beta W$]), where

$$W = -\beta[(E_{new} - E_{old}) + P(V_{new} - V_{old})] + N \ln(V_{new}/V_{old}), \tag{27}$$

and $\beta=1/(kT)$. The move was accepted if $W < 0$. If $W > 0$, a new random number ζ distributed in the interval (0,1) was generated and compared to exp($-\beta W$). The move was accepted if $\zeta < \exp(-\beta W)$ and rejected otherwise. Averages of different quantities such as the lattice energy, lattice dimensions, density, and the positions of the (T) are then determined. The fluctuations of a property A, defined as

$$F = \sqrt{\overline{A}^2 - (\overline{A})^2}, \tag{28}$$

will be reported with the averages for these simulations, as well as for the NPT-MD simulations described in succeeding text. In all the MC simulations, warm-up walks of 1,000–3,000 MC steps were done. The Markov walk was performed for a total number of steps varying from 100,000 at T=4.2 K to 250,000 at 300 K.

A problem of interest in NPT simulations is the evaluation of the average pressure. For a system of rigid polyatomic molecules, Smith [41, 42] has shown that the pressure can be calculated using the molecular virial theorem if the Hamiltonian of the system is rewritten in terms of the scaled coordinates of the molecular center of mass ($\mathbf{s}_i=\mathbf{r}_i/V^{1/3}$) and of the intramolecular distances relative to the center of mass ($\mathbf{d}_{i\alpha}=\mathbf{r}_{i\alpha}-\mathbf{r}_i$), invariant at volume scaling. A more general approach has been introduced by Parrinello and Rahman [43], who have used the full microscopic stress tensor for an N-particle system in a periodically repeating MD cell. Nose′ and Klein [44] have extended the calculation of the stress tensor to include the long-range Coulombic interactions and have applied this to rigid polyatomic molecules. We present in the Appendix a generalization of the treatment based on the accelerated convergence technique given by Karasawa and Goddard [18], to formulate the stress tensor for both the Coulombic and dispersion potentials assuming a system of rigid molecules in a periodic lattice. The calculated pressure, as given in equation (A9), has been used to provide an independent verification of the reliability of the codes developed in this study.

3.3 NPT Molecular Dynamics Calculations. The intermolecular interaction potential for RDX was subjected to a final and more rigorous test: NPT molecular dynamics simulations, in which there are no constraints other than the assumption of rigid-body molecules. Single trajectories at 4.2, 100, 200, 250, 273.15, 300, and 325 K and zero pressure were integrated for at least 10 ps. The calculations were performed using the MDSCPC4 set of programs [45]. In this procedure, the equations of motion for both the molecules and the simulation cell are integrated using a fifth-order Gear predictor-corrector [46]. The rotational motion is handled using the Evans quaternion algorithm [47] with a fifth-order Gear integrator. The algorithms used are described in detail in Nose′ and Klein [44]. A fixed time step of 2.0×10^{-15} s was used. The system consists of a box containing 27 unit cells [a 3×3×3 box of unit cells]. At the beginning of each simulation, the unit cells are identical to the experimental structure at T=300 K, 1 atm [2].

The initial velocities of the centers-of-mass of the molecules were selected at random, but subject to the following conditions: the translational and rotational velocities were selected such that the simulation cell had no bulk motion. Also the translational and rotational velocities were scaled to yield the desired temperature. The system was first integrated for 2,000 steps (4 ps) under conditions of constant volume in order to relax the system away from the initial state. During this period, the velocities were scaled at every five steps in order that the internal temperature of crystal mimic the imposed temperature. And additional 3,000 steps (6 ps) were then integrated (at constant volume) without additional scaling of the velocities. Finally, the isothermal-isobaric trajectory was integrated for at least 5,000 steps (10 ps) for each temperature at zero pressure. During the first 2,000 steps (4 ps) of each NPT trajectory, the velocities were scaled at every 5 steps as described previously. Averages were obtained from properties calculated at subsequent integration steps in the NPT simulation.

Summations given in equations (13)–(19) were adapted for inclusion of minimum-image periodic boundary conditions in all dimensions in these simulations [19]. The interactions are determined between the sites (atoms) in the simulation box and the nearest-image sites within the cutoff distance. In these calculations, the sum over reciprocal vectors was included for the Coulombic interactions, subject to the summation limit given by $(m_1^2 + m_2^2 + m_3^2) \leq 12^2$ (see equation [4]). Long-range corrections for the potential energy and virial contribution due to dispersion were calculated using the standard techniques [19]. The cutoff distance here is 80% of one-half the shortest perpendicular distance between two faces of the simulation cell, assuming unit cell sizes measured at 300 K, 1 atm [2]. This corresponds to a cutoff distance of 12.8508 Å. We monitored the simulation box size to be certain that the shortest perpendicular distance between two opposite faces of the box never became less than twice the cutoff distance to avoid violating the minimum image condition during the simulation [19].

4. RESULTS AND DISCUSSIONS

4.1 Molecular Packing Calculations. The results of the molecular packing calculations are given in Table 3. In the full minimization of the RDX crystal energy, the space symmetry is maintained with less than 0.003° deviations of the lattice angles from experiment. Also, the

maximum deviation of the fractional coordinates of the centroids [35] is 0.006. The deviation of the Euler angles from experiment is no greater than 1.183°.

Since accelerated convergence is not used for evaluation of the $1/r^6$ attractive terms in the nonbonded potential in the full minimization of the RDX crystal energy, dependence of the lattice energy on the cutoff distance is expected. This is shown (see Table 3) by results obtained for different Q parameters. For values of Q larger than 10, a small influence on the total energy per molecule and almost no effect on geometrical parameters of the lattice are found. In addition, these results are in very good agreement with those obtained by using the symmetry constraints procedure and accelerated convergence technique.

4.2 Symmetry-Constrained NPT Monte Carlo Calculations. Ideally, the structure predicted in a crystal-packing calculation should reproduce the crystal structure at temperatures close to 0 K. Although experimental data in this temperature region or extrapolated values from experiments performed at much higher temperatures are not available, we have performed NPT-MC calculations at 4.2 K to provide this comparison. Additionally, we investigated the influence of thermal effects on the crystallographic structure by performing MC calculations in the NPT ensemble at temperatures of T=100, 200, and 300 K and pressures of 1 atm and 500 atm. The averages and fluctuations corresponding to lattice constants, lattice potential energy, density, and the positions and orientation of the molecule in the asymmetric unit are given in Table 4.

As evident in Table 4, the effect caused by the increase in temperature from 4.2 K to 300 K at 1 atm is the expansion of the lattice dimensions. The most significant increase of 0.53 Å takes place in a direction parallel to the l_3 axis over this temperature range. Correspondingly, the overall density of the crystal decreases from 1.796 g/cm^3 at 4.2 K to 1.689 g/cm^3 at T=300 K. A similar trend is observed for calculations at P=500 atm. The unit cell dimensions are within 4% of the experimental values at T=300 K and 1 atm, with the largest deviation being the 1_3 parameter, which is 0.43 Å larger than the experimental value.

Table 4. NPT Monte Carlo Averages

				Unit Cell Dimensions			Center-of-Mass Fractionals			Quaternions				Euler Angles (X Convention) [44]		
T (K)	No. steps (10^3)	E (kJ/mol)	Density (g/cm^3)	l_1 (Å)	l_2 (Å)	l_3 (Å)	sx	sy	sz	q_0	q_1	q_2	q_3	Φ (°)	Θ (°)	Ψ (°)
Pressure = 1 atm																
4.2	100	-129.96	1.796	13.288 (0.038)	11.651 (0.038)	10.610 (0.038)	0.07635 (0.0009)	0.40714 (0.0014)	0.34670 (0.0015)	0.60974 (0.0030)	0.73574 (0.0021)	0.25980 (0.0037)	0.13917 (0.0028)	32.3	102.6	-6.6
100	205	-126.24	1.768	13.330 (0.199)	11.709 (0.205)	10.693 (0.203)	0.07653 (0.0043)	0.40502 (0.0074)	0.34847 (0.0083)	0.61160 (0.0165)	0.73461 (0.0116)	0.25622 (0.0203)	0.13999 (0.0149)	32.1	102.2	-6.3
200	210	-121.24	1.729	13.362 (0.326)	11.765 (0.342)	10.855 (0.408)	0.07642 (0.0070)	0.40035 (0.0141)	0.35315 (0.0162)	0.61637 (0.0293)	0.73140 (0.0212)	0.24832 (0.0364)	0.14171 (0.0275)	31.7	101.4	-5.8
300	250	-115.2	1.682	13.363 (0.492)	11.789 (0.520)	11.137 (0.731)	0.07545 (0.0121)	0.39350 (0.0212)	0.35883 (0.0232)	0.61681 (0.0511)	0.72934 (0.0320)	0.23554 (0.0677)	0.14692 (0.0504)	31.0	101.5	-4.3
Pressure = 500 atm																
4.2	100	-129.94	1.803	13.278 (0.038)	11.639 (0.037)	10.593 (0.038)	0.07625 (0.0009)	0.40738 (0.0014)	0.34643 (0.0015)	0.60957 (0.0029)	0.73571 (0.0021)	0.26041 (0.0036)	0.13899 (0.0027)	32.3	102.6	-6.6
100	200	-126.31	1.775	13.323 (0.199)	11.693 (0.201)	10.673 (0.204)	0.07644 (0.0043)	0.40522 (0.0075)	0.34821 (0.0084)	0.61162 (0.0163)	0.73455 (0.0114)	0.25661 (0.0202)	0.13963 (0.0145)	32.1	102.2	-6.4
200	210	-121.81	1.741	13.359 (0.309)	11.752 (0.323)	10.794 (0.352)	0.07650 (0.0067)	0.40175 (0.0123)	0.35162 (0.0143)	0.61516 (0.0262)	0.73212 (0.0187)	0.25069 (0.0336)	0.14124 (0.0249)	31.8	101.6	-6.0
300	250	-115.94	1.694	13.369 (0.459)	11.804 (0.495)	11.036 (0.640)	0.07559 (0.0104)	0.39568 (0.0201)	0.35689 (0.0223)	0.61658 (0.0425)	0.72984 (0.0292)	0.24020 (0.0570)	0.14684 (0.0447)	31.6	101.0	-4.8
Experiment (1 atm)																
300			1.806	13.182	11.574	10.709	0.08171	0.40516	0.3512	0.61663	0.73049	0.25575	0.14398	32.4	101.4	-6.2

No significant deviations of the position and orientation of molecule (T) from the experimental values were observed for this range of temperatures and pressures. We found that the maximum deviations of the average values of the fractional coordinates and Euler angles from the experimental data are smaller than 0.006 and 2°, respectively.

4.3 NPT Molecular Dynamics Calculations. Averages and fluctuations of crystal structure information calculated from the trajectories integrated at T=4.2 and 300 K are given in Table 5. These averages include lattice dimensions, mass-center fractionals, and Euler angles of the eight molecules of the unit cell. The averages for each of the eight molecules in the unit cell are over the 27 unit cells within the simulation box. The results at 4.2 K are in close agreement with the molecular packing and symmetry-constrained NPT-MC results.

The time histories of the lattice parameters (l_1, l_2, l_3, α, β, and γ) and the volume, pressure, and rotational and translational temperatures for the T=300 K trajectory are given in Figures 3 and 4. The trajectory is well behaved; each property oscillates about the average value given in Table 5 for the duration of the trajectory. The lattice dimensions deviate no more than 2% from the experimental values. The l_3 prediction is in much better agreement with experiment (within 0.02 Å) than the predictions of the NPT-MC calculations. Figure 5 provides a comparison with experiment [2] of the averages of orientational parameters of the eight molecules in the unit cell. It is evident that rotational disorder is small and the center-of-mass positions of the molecules are very close to those determined experimentally [2].

Trajectories at T=100, 200, 250, 273.15, 293, and 325 K were also integrated for 10 ps to provide information on the behavior of the system with increasing temperature. Averages of the lattice dimensions resulting from these simulations are given in Table 6. This information can be used to extract the thermal expansion coefficients by using the relations:

$$\alpha \equiv \frac{1}{X}\left(\frac{\partial X}{\partial T}\right)_P, \tag{29}$$

Table 5. NPT-MD Averages[a] for T=4.2 amd 300 K

Center-of-Mass Fractionals

	Sx			Sy			Sz		
	NPT MD 4.2 K	NPT MD 300 K	Expt. [2] 300 K	NPT MD 4.2 K	NPT MD 300 K	Expt. [2] 300 K	NPT MD 4.2 K	NPT MD 300 K	Expt. [2] 300 K
1	0.076361 (0.000941)	0.077008 (0.009010)	0.081715	0.407179 (0.001116)	0.404727 (0.009104)	0.405161	0.346661 (0.001327)	0.348667 (0.011963)	0.352120
2	0.576355 (0.000999)	0.576897 (0.008687)	0.581715	0.092817 (0.001118)	0.095245 (0.009633)	0.094839	0.653332 (0.001276)	0.651197 (0.013111)	0.647880
3	0.923637 (0.000938)	0.922984 (0.009099)	0.918285	0.907181 (0.001182)	0.904913 (0.009464)	0.905161	0.153362 (0.001263)	0.151646 (0.011795)	0.147880
4	0.423646 (0.000936)	0.423024 (0.008698)	0.418285	0.592823 (0.001085)	0.595367 (0.009440)	0.594839	0.846645 (0.001311)	0.848562 (0.013043)	0.852120
5	0.923446 (0.000893)	0.923097 (0.008804)	0.918285	0.592823 (0.001070)	0.595295 0.009361)	0.594839	0.653356 (0.001283)	0.651597 (0.011891)	0.647880
6	0.423637 (0.000968)	0.423156 (0.008669)	0.418285	0.907175 (0.001074)	0.904666 (0.008781)	0.905161	0.346639 (0.001267)	0.348421 (0.013482)	0.352120
7	0.076354 (0.000970)	0.077073 (0.008668)	0.081715	0.092824 (0.001122)	0.095218 (0.009666)	0.094839	0.846669 (0.001286)	0.848568 (0.012020)	0.852120
8	0.576366 (0.000981)	0.576761 (0.009304)	0.581715	0.407179 (0.001051)	0.404569 (0.009371)	0.405161	0.153335 (0.001251)	0.151343 (0.012859)	0.147880

[a] Fluctuations [Eq. (28)] of MD-NPT predictions in parentheses.

Table 5. NPT-MD Averages[a] for T=4.2 amd 300 K (continued)

Euler Angles (X-Convention [44])

	Φ (°)			Θ (°)			Ψ (°)		
	NPT MD 4.2 K	NPT MD 300 K	Expt. [2] 300 K	NPT MD 4.2 K	NPT MD 300 K	Expt. [2] 300 K	NPT MD 4.2 K	NPT MD 300 K	Expt. [2] 300 K
1	32.3 (0.3)	32.2 (2.6)	32.4	102.6 (0.3)	102.3 (2.9)	101.4	-6.6 (0.3)	-6.3 (2.6)	-6.2
2	147.7 (0.3)	147.8 (2.6)	147.6	77.4 (0.3)	77.8 (3.0)	78.6	173.4 (0.3)	173.7 (2.6)	173.8
3	-32.3 (0.3)	-32.3 (2.7)	-32.4	77.4 (0.3)	77.7 (3.0)	78.6	173.4 (0.3)	173.8 (2.7)	173.8
4	-147.7 (0.3)	-147.8 (2.7)	-147.6	102.6 (0.3)	102.2 (3.0)	101.4	-6.6 (0.3)	-6.2 (2.7)	-6.2
5	32.3 (0.3)	32.2 (2.6)	32.4	102.6 (0.3)	102.2 (3.0)	101.4	-6.6 (0.3)	-6.3 (2.6)	-6.2
6	147.7 (0.3)	147.8 (2.7)	147.6	77.4 (0.3)	77.8 (3.0)	78.6	173.4 (0.3)	173.8 (2.7)	173.8
7	-32.3 (0.3)	-32.3 (2.7)	-32.4	77.4 (0.3)	77.7 (3.0)	78.6	173.4 (0.3)	173.7 (2.7)	173.8
8	-147.7 (0.3)	-147.8 (2.6)	-147.6	102.6 (0.3)	102.3 (3.0)	101.4	-6.6 (0.3)	-6.3 (2.6)	-6.2

[a] Fluctuations [Eq. (28)] of MD-NPT predictions in parentheses.

27

Table 5. NPT-MD Averages[a] for T=4.2 amd 300 K (continued)

Lattice Dimensions of the Unit Cell

T(K)	l_1 (Å)		l_2 (Å)		l_3 (Å)		Volume (Å^3)	
	Calculated	Expt. [2]	Calculated	Expt. [2]	Calculated	Expt. [2]	Calculated	Expt. [2]
4.2	13.290 (5.2×10^{-4})		11.654 (2.0×10^{-3})		10.610 (7.4×10^{-4})		1642.999	
300	13.396 (0.0104)	13.182	11.798 (0.0101)	11.574	10.732 (0.0120)	10.709	1696.150	1633.856

[a] Fluctuations [Eq. (28)] of MD-NPT predictions in parentheses.

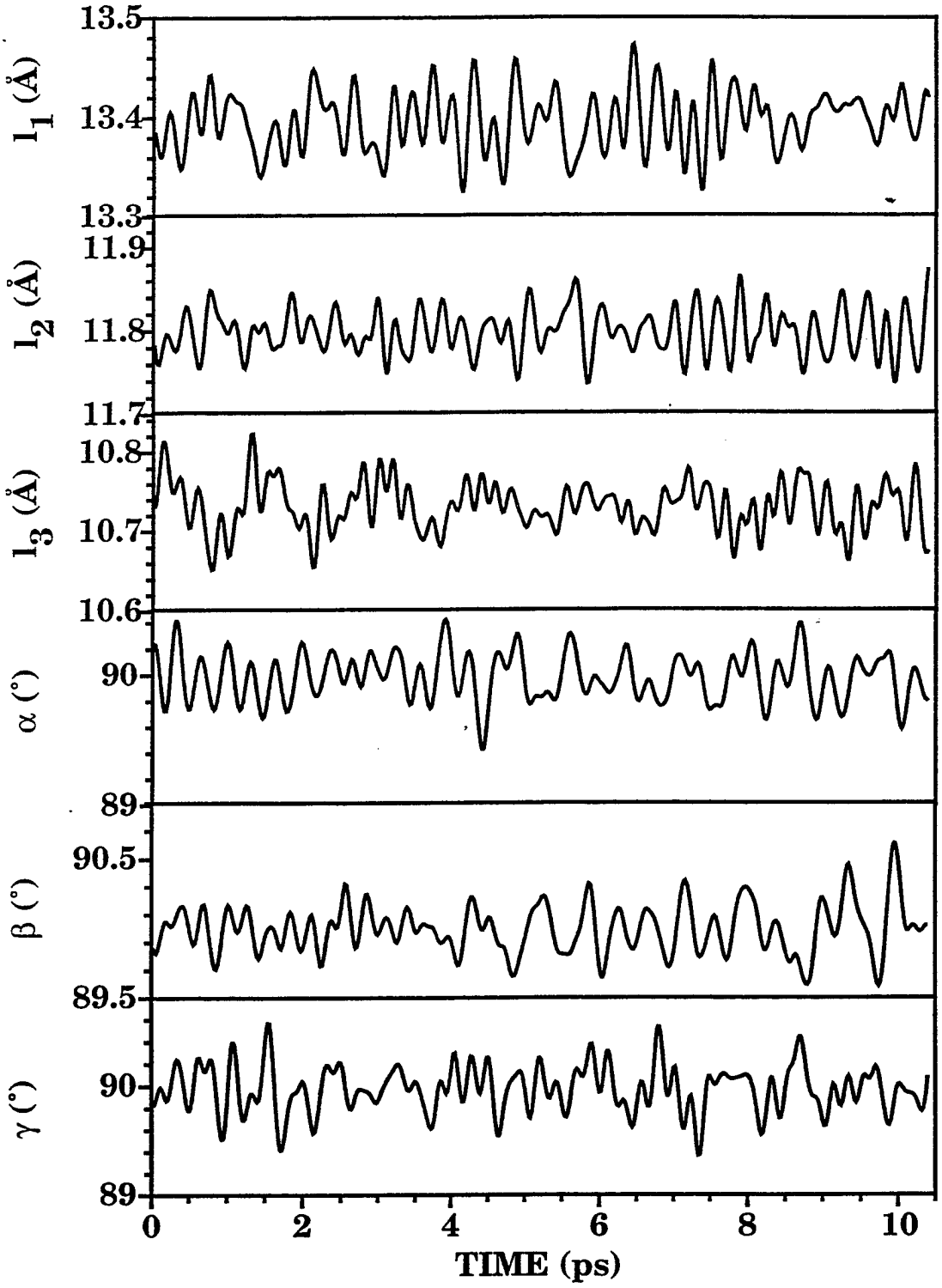

Figure 3. Time histories of lattice parameters (1_1, 1_2, 1_3, α, β, γ) for isothermal-isobaric trajectory corresponding to T=300 K, 0 atm.

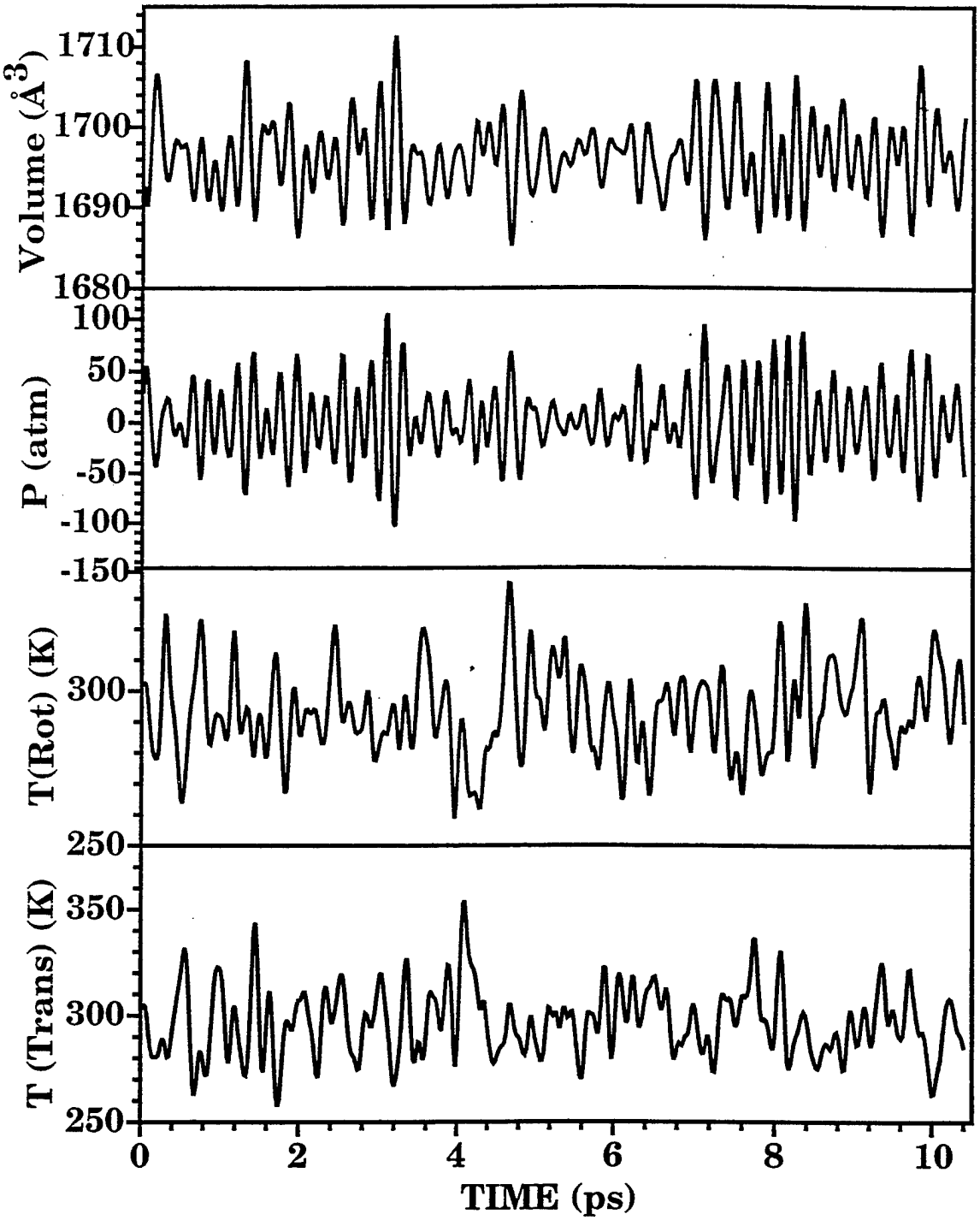

Figure 4. Time histories of unit cell volume, pressure, rotational temperature (T[Rot]), and center-of-mass translational temperature (T[trans]) for isothermal-isobaric trajectory corresponding to T=300 K, 0 atm.

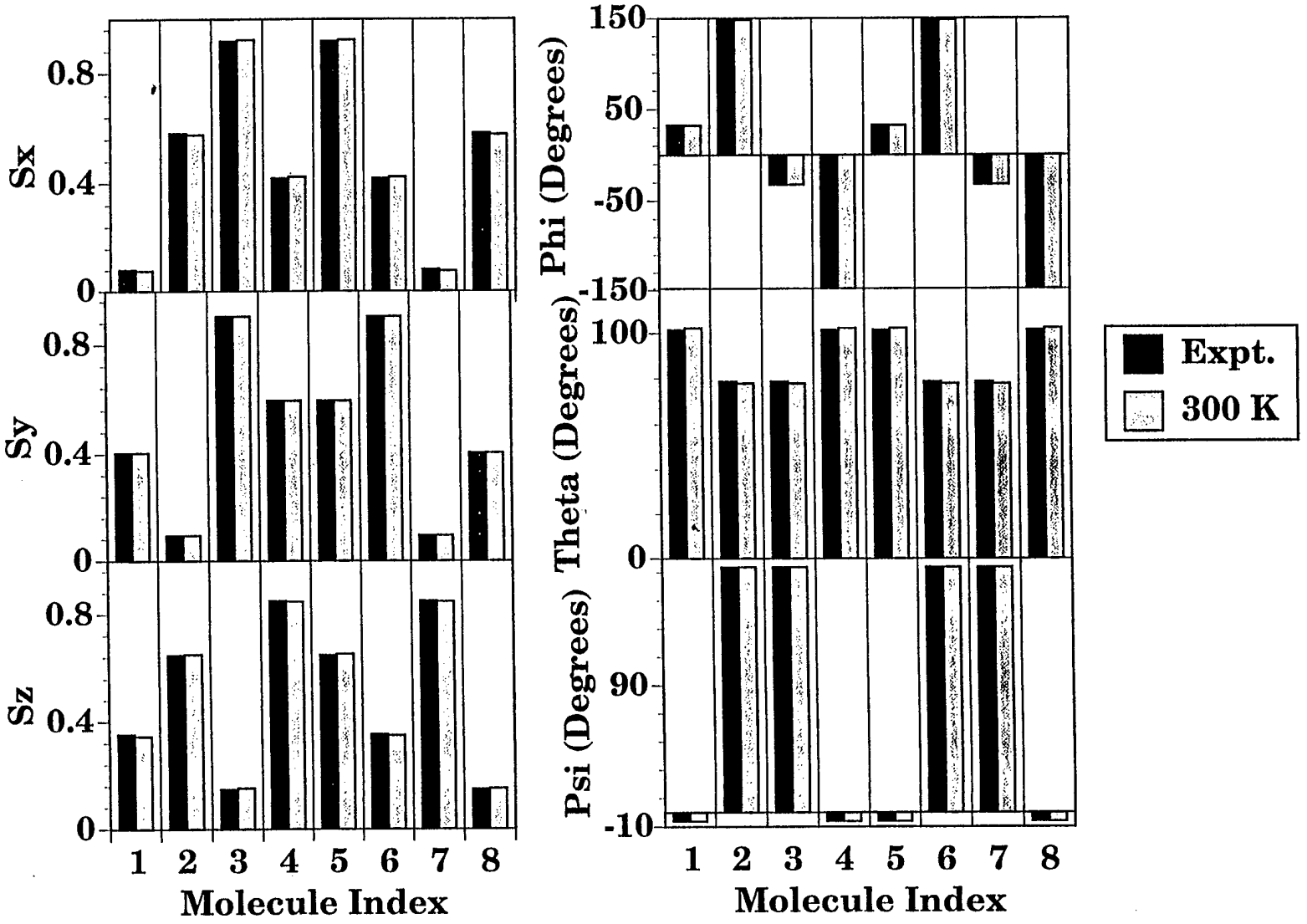

Figure 5. Comparison of time-averaged center-of-mass fractional positions and Euler angles (X-Convention) with experiment at T=300 K, 0 atm.

Table 6. NPT-MD Lattice Dimensions vs. Temperature

Lattice Dimensions

T(K)	l_1 (Å)	l_2 (Å)	l_3 (Å)	Volume (Å^3)
	Calculated	Calculated	Calculated	Calculated
4.2	13.290	11.654	10.610	1643.294
100	13.321	11.699	10.646	1659.098
200	13.360	11.748	10.683	1676.732
250	13.385	11.771	10.710	1687.412
273.15	13.389	11.788	10.726	1692.880
293	13.394	11.796	10.731	1695.451
300	13.396	11.798	10.732	1696.150
325	13.416	11.815	10.750	1703.983

Coefficients of Fit of Lattice Parameters to Quadratic in Temperature

Parameter[a]	l_1	l_2	l_3	Volume
A	6.307055×10^{-6}	-1.512549×10^{-7}	8.828888×10^{-7}	9.259430×10^{-4}
B	-3.229344×10^{-3}	6.484753×10^{-4}	-1.068887×10^{-5}	-3.228835×10^{-1}
C	13.79879	11.61935	10.65897	1710.723

[a] A, B, and C in units of Å/T^2, Å/T, and Å, respectively for l_i, i=1, 2, and 3.
A, B, and C in units of Å^3/T^2, Å^3/T, and Å^3, respectively for the volume.

where α is the coefficient of linear expansion of the material and X denotes the length of one of the sides of the unit cell. The coefficient of volume expansion, β, has a similar form:

$$\beta \equiv \frac{1}{V}\left(\frac{\partial V}{\partial T}\right)_P . \qquad (30)$$

A single value of the linear expansion coefficient at T=293 K (63.6×10^{-6} K^{-1}) has been reported [49], which implies that thermal expansion is the same in each of the three dimensions. Two volume expansion coefficients, 191×10^{-6} K^{-1} at 293 K and 250×10^{-6} K^{-1} for the temperature range 293–373 K, are also given. Figure 6 shows the unit-cell lattice parameters and volume as functions of temperature. The squares denote the time-averaged values obtained from the trajectories (listed in Table 6), and the lines denote fits of these averages to quadratic functions of temperature over the range 250 to 325 K. The coefficients of each fit are given in Table 6. The fits can be used to evaluate equations (29) and (30) to provide the linear and volume expansion coefficients for this model. The linear expansion coefficients for lattice dimensions l_1, l_2, and l_3 are 34.8×10^{-6}, 47.5×10^{-6}, and 47.2×10^{-6} K^{-1}, which are 45, 25, and 26% smaller than the experimental values, respectively. The results of the simulations differ from the experimental values in that the value of the linear expansion coefficient for cell parameter l_1 is smaller than those for cell parameters l_2 and l_3, which are approximately the same. The calculated value of the volume expansion coefficient (129.6×10^{-6} K^{-1}) at 293 K is 32% smaller than the measured value [49].

5. SUMMARY AND CONCLUSIONS

In this paper, we have developed an intermolecular potential for the RDX crystal based on 6-exp Buckingham potentials terms plus Coulombic interactions. Electrostatic charges of different atoms in the RDX molecule were determined from fits to *ab initio* electrostatic potentials calculated at the MP2/6-31G** level. Values for heteroatom potential parameters were obtained from those for homoatom parameters by using traditional combination rules. Values for several of the homoatom parameters were taken from published data [10, 30], including the H-H and C-C potential terms. The published value of the B parameter of the 6-exp Buckingham potential for the N-N and O-O Buckingham terms was used, and the values of the remaining A and C parameters for these homonuclear interactions were optimized by nonlinear least-squares fitting of the potential to a general function that represents a weighted superposition of forces and torques plus the square of the differences between the predicted and experimental

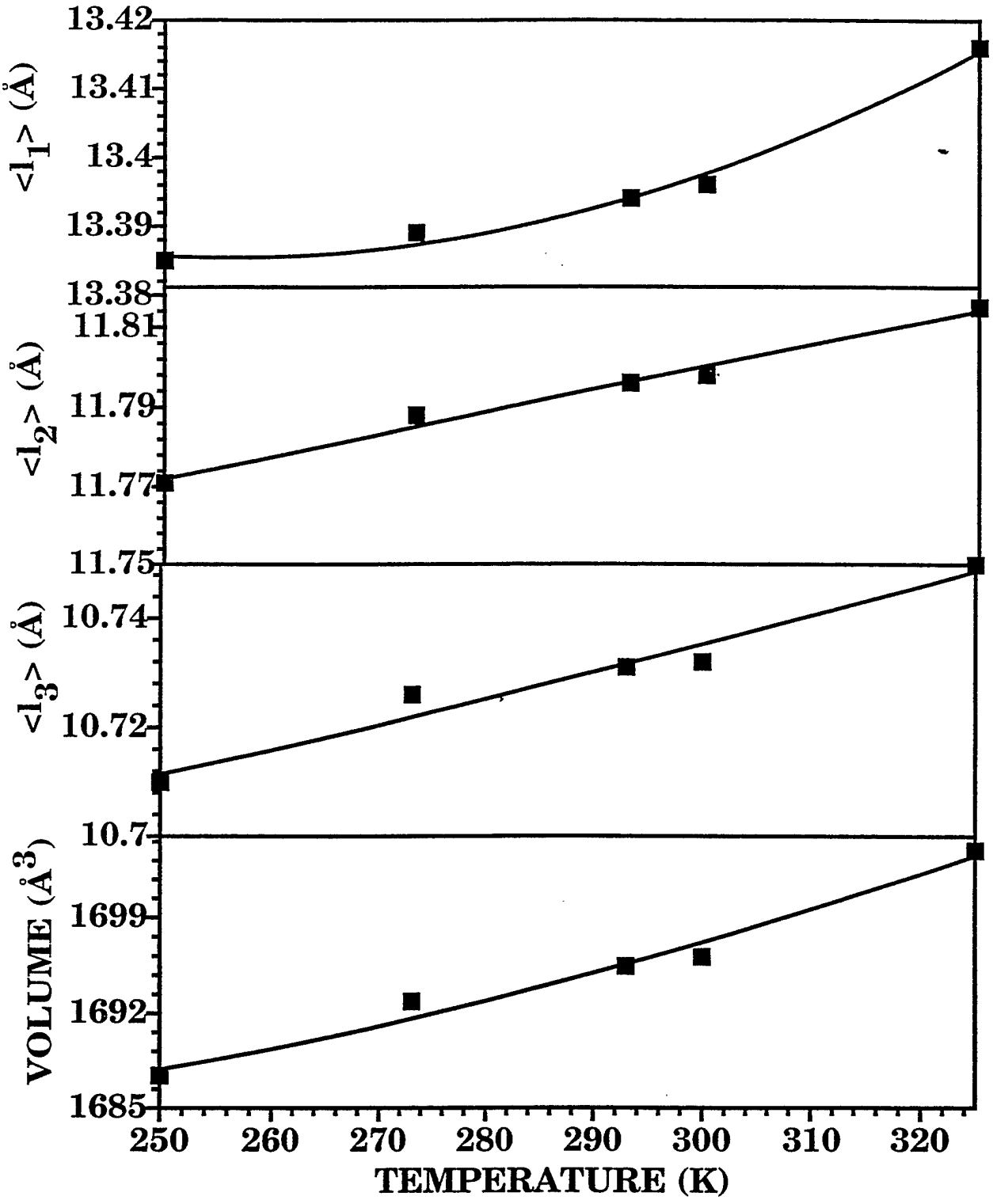

Figure 6. Lattice parameters (1_1, 1_2, 1_3,) and unit cell volume as a function of temperature.

lattice energies for the experimentally determined crystal structure. The potential parameters were adjusted to reproduce the experimentally determined space group symmetry, the lattice dimensions for the RDX crystal, and the enthalpy of sublimation.

Accurate values of the crystal lattice energy have been obtained in symmetry-constrained molecular packing and NPT-MC calculations by employing the technique of accelerated convergence for the dispersion and Coulombic lattice sums. Molecular packing calculations with and without symmetry constraints indicate very good agreement with experimental geometrical and thermochemical data.

The temperature dependencies of the physical parameters of the lattice have been investigated by performing symmetry-constrained NPT-MC calculations in the range 4.2–300 K and at pressures of 1 and 500 atm. The average values of the physical lattice parameters calculated from Markov walks with 100,000–250,000 steps indicate that the major modification of the lattice takes place along the l_3 axis with increasing temperature. Molecular reorientation and translation of the mass-center fractionals are no greater than 2° and 0.006 from the experimental values, respectively, over the temperature and pressure ranges considered. Lattice parameters calculated at T=300 K and 1 atm are within 4% of experimental values.

A final test of the interaction potential was performed using isothermal-isobaric molecular dynamics simulations at 0 pressure over the temperature range 4.2–325 K. The results of these calculations indicate that this model reproduces to within 2% the measured cell dimensions of the RDX crystal at 300 K. Additionally, little rotational or translational disorder occurred in the thermal, unconstrained trajectories.

Linear and volume expansion coefficients at 293 K were calculated using time averages over the temperature range 250–325 K. The calculations differ from experiment in that one of the dimensions of the unit cells does not have the same linear expansion coefficient as the other two dimensions, as implied by the single reported value [49] of the linear expansion coefficient. The linear expansion coefficients for the three dimensions are 45, 25, and 26% smaller than the

experimental value. The volume expansion coefficient is 32% smaller than the measured value [49].

These results demonstrate that the proposed potential provides an accurate description of the α-form of the RDX crystal. The structure resulting from NPT-MD simulations at 300 K and 0 pressure is in excellent agreement with measured structural information. The lack of rotational and translational disorder of the molecules seen in all of the simulations indicates that the interaction potential has the correct anisotropies of the intermolecular interactions. The good agreement of the thermal expansion coefficients with experiment at 293 K suggests that the model behaves properly over a large temperature range, even though thermal information was not used in the determination of the potential energy parameters.

This model appears to be useful for prediction of nonreactive processes occurring in an α-RDX crystal. Refinement of this model can be made by including the effects of intramolecular motions, particularly of low-frequency torsional motions of the nitro groups and the ring. In addition, the model can be extended to reproduce not only geometrical and energetic parameters, but also spectroscopic data for the RDX lattice. Extensions of the model to include the intramolecular degrees of freedom are expected to facilitate full atomistic investigations of the dynamics of this energetic material. Additionally, preliminary results indicate that the parameters determined for this potential energy function are transferable to other important cyclic nitramines.

6. REFERENCES

1. McCrone, W. C. Analytic Chemistry. Vol. 22, p. 954, 1950.

2. Choi, C. S., and E. Prince. Acta Crystallographa. Vol. B28, p. 2857, 1972.

3. Rogers, J. T. "Physical and Chemical Properties of RDX and HMX." Report No. HDC-20-P-26-SER-B, CPIA Abstract No. 73-1016, AD 904-410L, Holston Defense Corporation, Kingsport, TN, August 1962.

4. Pertsin, A. J., and A. I. Kitaigorododsky. The Atom-Atom Potential Method, Applications to Organic Molecular Solids. Berlin: Springer-Verlag, 1987.

5. Desiaju, G. R. Crystal Engineering: The Design of Organic Solids. Amsterdam: Elsevier, 1989.

6. Gavessotti, A., and G. Filippini. Acta Crystallographa. Vol. B49, p. 868, 1993.

7. Williams, D. E., and T. L. Starr. Computers and Chemistry. Vol. 1, p. 173, 1977.

8. Weiner, S. J., P. A. Kollman, D. T. Nguyen, and D. A. Case. Journal of Computational Chemistry, vol. 7, p. 230, 1986.

9. Nemethy, G., K. D. Gibson, K. A. Palmer, C. N. Yoon, G. Paterlini, S. Rumsey, and H. A. Scheraga. Journal of Physical Chemistry. Vol. 96, p. 6474, 1972.

10. Mayo, S. L., B. D. Olafson, and W. A. Goddard III. Journal of Physical Chemistry. Vol. 94, p. 8897, 1990.

11. Buckingham, A. D., and P. W. Fowler. Canadian Journal of Chemistry. Vol. 63, p. 2018, 1985.

12. Price, S. L., and A. J. Stone. Molecular Physics. Vol. 51, p. 569, 1987.

13. Willock, D. J., S. L. Price, M. Leslie, and C. R. A. Catlow. Journal of Computational Chemistry, vol. 16, p. 628, 1995.

14. Mirsky, K. Computing in Crystallography. Edited by H. Schenk, R. Olthof-Hazekamp, H. von Koningsveld, and G. C. Bassi, Delft, Netherlands: Delft University Press, p. 169, 1978.

15. Williams, D. E. Acta Crystallographa. Vol. A27, p. 452, 1977.

16. Williams, D. E. Crystal Cohesion and Conformational Energies. Edited by R. M. Metzger, Berlin: Springer-Verlag, pp. 3–40, 1981.

17. Nijboer, B. R. A., and F. W. Dewette. Physica. Vol. 23, p. 309, 1957.

18. Karasawa, N., and W. A. Goddard III. Journal of Physical Chemistry. Vol. 93, p. 7320, 1989.

19. Allen, M. P., and D. J. Tildesley. Computer Simulation of Liquid. New York: Oxford University Press, 1989.

20. Hsu, Leh-Yen, and D. E. Williams. Acta Crystallographa. Vol. A36, p. 277, 1980.

21. Giacovazzo, C. (ed.). Fundamentals of Crystallography. New York: Oxford University Press, 1992.

22. Rosen, J. M., and C. Dickinson. Journal of Chemistry and Engineering Data. Vol. 14, p. 120, 1963.

23. Wiberg, K. B., and P. R. Rablen. Journal of Computational Chemistry. Vol. 14, p. 1504 (and references therein), 1993.

24. Breneman, C. M., and K. B. Wiberg. Journal of Computational Chemistry. Vol. 11, p. 361, 1990.

25. Frish, M. J., G. W. Trucks, H. B. Schlegel, P. M. W. Gill, B. G. Johnson, M. A. Robb, J. R. Cheeseman, T. Keith, G. A. Patersson, J. A. Montgomery, K. Raghavachari, M. A. Al-laham, V. G. Zakrzewski, J. V. Ortiz, J. B. Foresman, J. Cioslowski, B. B. Stefanov, A. Nanyakkara, M. Challacombe, C. Y. Peng, P. Y. Ayala, W. Chen, M. W. Wong, J. L. Andres, E. S. Replogle, R. Gomperts, R. L. Martin, D. J. Fox, J. S. Binkley, D. J. Defrees, J. Baker, J. P. Stewart, M. Head-Gordon, C. Gonzales, and J. A. Pople. Gaussian 94. Revision C.3, Gaussian, Inc., Pittsburgh, PA, 1995.

26. Moller, C. M. S. Physical Review. Vol. 46, p. 618, 1934.

27. Hariharan, P. C., and J. A. Pople. Theoretica Chimica Acta. Vol. 28, p. 213, 1973.

28. Gordon, M. S. Chemical Physics Letters. Vol. 76, p. 163, 1980.

29. Williams, D. E. "PCK91, A Crystal Molecular Packing Analysis Program." Department of Chemistry, University of Louisville, Louisville, KY, 1991.

30. Williams, D. E., and D. J. Houpt. Acta Crystallographa. Vol. B42, p. 286, 1986.

31. Starr, T. L., and D. E. Williams. Acta Crystallographa. Vol. A33, p. 771, 1977.

32. Press, W. H., S. A. Teukolsky, W. T. Vetterling, and B. P. Flannery. Numerical Recipes. New York: Cambridge University Press, 1992.

33. Chirlian, L. E., and M. M. Francl. Journal of Computational Chemistry. Vol. 8, p. 894, 1987.

34. Hagler, A. T., S. Lifson, and P. Dauber. Journal of the American Chemical Society. Vol. 101, p. 5122, 1979.

35. Gibson, K. D., and H. A. Scheraga. Journal of Physical Chemistry. Vol. 99, p. 3752, 1995.

36. Gay, D. M. ACM Transaction of Mathematics Software. Vol. 9, p. 503, 1983.

37. Gibson, K. D., and H. A. Scheraga. "LMIN: A Program for Crystal Packing." QCPE No. 664.

38. Hahn, T. International Tables for Crystallography. Boston: Reidel, Dordrecht, 1983.

39. Evans, D. Molecular Physics. Vol. 34, p. 317, 1977.

40. Rice, B. M., W. Mattson, J. Grosh, and S. F. Trevino. Physical Review. Vol. E53, p. 611, 1996.

41. Smith, W. Information Quarterly for Computer Simulation of Condensed Phases: The CCP5 Newsletter. Vol. 26, p. 43, 1987.

42. Smith, W. Information Quarterly for Computer Simulation of Condensed Phases: The CCP5 Newsletter. Vol. 39, p. 14, 1993.

43. Parrinello, M., and A. Rahman. Physical Review of Letters. Vol. 45, p. 1196, 1980.

44. Nose′, S., and M. L. Klein. Molecular Physics. Vol. 50, p. 1055, 1983.

45. Smith, W. MDCSPC, Version 4.3, A Program for Molecular Dynamics Simulations of Phase Changes. CCP5 Program Library, SERC, May 1991.

46. Gear, C. W. Numerical Initial Value Problems in Ordinary Differential Equations. Englewood Cliffs, NJ: Prentice-Hall, 1971.

47. Evans, D. J., and S. Murad. Molecular Physics. Vol. 34, p. 327, 1977.

48. Goldstein, H. Classical Mechanics. Reading, MA: Addison-Wesley, 1980.

49. Dobratz, M. "Properties of Chemical Explosives and Explosive Simulants." Report No. UCRL-52997, Lawrence Livermore National Laboratory, Livermore, CA, pp. 19–131 and 19–132, March 1981.

INTENTIONALLY LEFT BLANK.

APPENDIX:

FORMULATION OF THE STRESS TENSOR

INTENTIONALLY LEFT BLANK.

It has been previously shown that for a system of rigid molecules in a periodic system under external pressure that the internal stress tensor Π can be defined as[1]

$$\Pi_{\varepsilon\gamma} = \frac{1}{V}\left[\sum_{i=1}^{N} m_i(\vec{\mathbf{h}}\dot{\mathbf{s}}_i)_\varepsilon^t\,(\vec{\mathbf{h}}\dot{\mathbf{s}}_i)_\gamma + \sum_\eta \frac{-\partial\Phi}{\partial h_{\varepsilon\eta}} h_{\gamma\eta}\right], \tag{A1}$$

where Φ is the potential energy between the molecules in the central cell and the molecules in the rest of the crystal. Here we have assumed the Cartesian coordinates of the atom α belonging to molecule of index i are represented as functions of the molecular mass center, $\vec{\mathbf{h}}\mathbf{s}_i$, and the intramolecular distance, $\mathbf{d}_{i\alpha}$:

$$\mathbf{r}_{i\alpha} = \vec{\mathbf{h}}\mathbf{s}_{i\alpha} = \vec{\mathbf{h}}\mathbf{s}_i + \mathbf{d}_{i\alpha}, \tag{A2}$$

where $\mathbf{s}_{i\alpha}$ and $\mathbf{s}_i$ are the fractional vectors of the atom (i,α) and of the molecule i, respectively, and $\vec{\mathbf{h}} = [\mathbf{l}_1,\mathbf{l}_2,\mathbf{l}_3]$ is the matrix of basis vectors.

In this appendix we give the expressions of the Coulombic and dispersion stress tensor. These results are obtained following the method originally introduced by Nose′ and Klein[1] for the case of Coulombic interactions. The corresponding contribution of the repulsive energy (equation [6] in the report) to the stress tensor is calculated only in the real space as

$$V\Pi_{rep\varepsilon\gamma} = \frac{1}{2}\sum_{\mathbf{n}}^{\infty *}\sum_{i=1}^{N}\sum_{\alpha=1}^{n_i}\sum_{j=1}^{N}\sum_{\beta=1}^{n_i} A_{i\alpha j\beta}B_{i\alpha j\beta}\exp(-B_{i\alpha j\beta}r_{ni\alpha j\beta})(\mathbf{r}_{ni\alpha j\beta})_\varepsilon(\mathbf{r}_{nij})_\gamma. \tag{A3}$$

---

[1] Nose′, S., and M. L. Klein. Molecular Physics. Vol. 50, p. 1055, 1983.

Using the identities $\partial V/\partial h_{\varepsilon\eta} = V h^{-1}_{\eta\varepsilon}$ and $\partial h^{-1}_{\mu\nu} / \partial h_{\varepsilon\eta} = h^{-1}_{\mu\varepsilon} h^{-1}_{\nu\eta}$, the Coulombic stress tensor is found to be of the form $\Pi^1 = \Pi^1_{dir} + \Pi^1_{rec}$, where

$$V\Pi^1_{dir\,\varepsilon\gamma} = \frac{1}{2} \sum_{\mathbf{n}}^{\infty} {}^{*} \sum_{i=1}^{N} \sum_{\alpha=1}^{n_i} \sum_{j=1}^{N} \sum_{\beta=1}^{n_j} q_{i\alpha} q_{j\beta} \frac{(\mathbf{r}_{ni\alpha j\beta})_\varepsilon (\mathbf{r}_{nij})_\gamma}{r^3_{ni\alpha j\beta}} \left[\mathrm{erfc}(a_1) + \frac{2 r_{ni\alpha j\beta}}{\sqrt{\pi}\eta_1} \exp(-a_1^2) \right], \qquad \text{(A4)}$$

and

$$V\Pi^1_{rec\,\varepsilon\gamma} = \frac{1}{2\pi V} \sum_{\mathbf{k}_m \neq 0} \frac{\exp(-b_1^2)}{k_m^2} \left\{ |S_1(\mathbf{k}_m)|^2 \left[\delta_{\varepsilon\gamma} - 2 \frac{(1 + \pi^2 \mathbf{k}_m^2 / \eta_1^2)}{\mathbf{k}_m^2} (\mathbf{k}_m^2)_\varepsilon (\mathbf{k}_m^2)_\gamma \right] \right.$$

$$- \sum_{\mathbf{n}}^{\infty} {}^{*} \sum_{i=1}^{N} \sum_{\alpha=1}^{n_i} q_{i\alpha} 2\pi i (\mathbf{k}_m)_\varepsilon (\mathbf{d}_{i\alpha})_\gamma \left[S_1(\mathbf{k}_m) \exp(-2\pi i \mathbf{k}_m \mathbf{r}_{i\alpha}) \right.$$

$$\left. \left. - S_1(-\mathbf{k}_m) \exp(2\pi i \mathbf{k}_m \mathbf{r}_{i\alpha}) \right] \right\}. \qquad \text{(A5)}$$

For flexible molecules, an additional term representing the contribution of the potential term E^1_{cor} should be included (see, for example, Essman et al.[2]).

Similarly, the stress terms determined by the dispersion potential are calculated as:

[2] Essmann, U., L. Perera, M. L. Berkowitz, T. Darden, H. Lee, and L. G. Pedersen. Journal of Chemical Physics. Vol. 103, p. 8577.

$$\Pi^{1}_{dir\,\varepsilon\gamma} = \frac{1}{2}\sum_{\mathbf{n}}^{\infty *}\sum_{i=1}^{N}\sum_{\alpha=1}^{n_i}\sum_{j=1}^{N}\sum_{\beta=1}^{n_j} C_{i\alpha j\beta}\,\frac{\exp(-a_6^2)}{r_{ni\alpha j\beta}^{8}}\,(6+6a_6^2+3a_6^4+a_6^6)(\mathbf{r}_{ni\alpha j\beta})_\varepsilon(\mathbf{r}_{nij})_\gamma, \qquad (A6)$$

$$\Pi^{6}_{rec\,\varepsilon\gamma} = \frac{\pi^{9/2}}{3V}\sum_{\mathbf{k}_m\neq 0}|S_6(\mathbf{k}_m)|^2\left\{k_m^3\left[\sqrt{\pi}\,\mathrm{erfc}(b_6)+\left(\frac{1}{2b_6^3}-\frac{1}{b_6}\right)\exp(-b_6^2)\right]\delta_{\varepsilon\gamma}\right.$$

$$\left. + 3k_m\left[\sqrt{\pi}\,\mathrm{erfc}(b_6)-\exp(-b_6^2)/b\right](\mathbf{k}_m)_\varepsilon(\mathbf{k}_m)_\gamma\right\}$$

$$-\frac{\pi^{9/2}}{3V}\sum_{\mathbf{n}}^{\infty *}\sum_{i=1}^{N}\sum_{\alpha=1}^{n_j}(C_{i\alpha i\alpha})^{1/2}k_m^3\left[\sqrt{\pi}\,\mathrm{erfc}(b_6)+\left(\frac{1}{2b_6^3}-\frac{1}{b_6}\right)\right]2\pi i(\mathbf{k}_m)_\varepsilon(\mathbf{d}_{i\alpha})_\gamma$$

$$\times\sum_{\mathbf{k}_m\neq 0}\left(S_1(\mathbf{k}_m)\exp(-2\pi i\mathbf{k}_m\mathbf{r}_{i\alpha})-S_1(-\mathbf{k}_m)\exp(2\pi i\mathbf{k}_m\mathbf{r}_{i\alpha})\right). \qquad (A7)$$

and

$$\Pi^{6}_{cor\,\varepsilon\gamma} = \frac{\pi^{3/2}\eta_6^3}{6V}\left[\sum_{i=1}^{N}\sum_{\alpha=1}^{n_i}(C_{i\alpha i\alpha})^{1/2}\right]^2\delta_{\varepsilon\gamma}. \qquad (A8)$$

In this case, there is a nonzero contribution of the potential term E^6_{cor} to the stress tensor, due to the volume dependence of the first term in equation (19). In the previously listed expressions, indices α and β denote different molecules of the ensemble, while indices ε and γ represent the x, y, and z components of the tensor, and δ is the Dirac delta function.

Under hydrostatic conditions, at equilibrium, the pressure in the system can be calculated as 1/3 of the average of the trace of the total stress tensor:

$$P = \frac{1}{3V}\left\langle \sum_{i=1}^{N}\frac{\mathbf{P}_i^2}{m_i} + (\Pi_{xx}^{tot} + \Pi_{yy}^{tot} + \Pi_{zz}^{tot})\right\rangle, \qquad \text{(A9)}$$

where the total contributions from repulsive, dispersion, and Coulombic potential terms are included in the stress tensorial terms $\Pi_{\varepsilon\gamma}^{tot}$.

Using the identity $\partial V/\partial h_{\varepsilon\eta} = Vh_{\eta\varepsilon}^{-1}$ with the general definition (A1), it follows that at equilibrium and under hydrostatic conditions, an alternative formulation of the pressure is

$$P = \frac{1}{3V}\left\langle \sum_{i=1}^{N}\frac{P_i^2}{m_i} - 3V\frac{\partial\Phi\left[(V^{1/3}\mathbf{r})^N\right]}{\partial V}\right\rangle. \qquad \text{(A10)}$$

This expression has been previously used by Smith[3, 4] for calculating the pressure in a molecular system that can expand or contract isotropically.

---

[3] Smith, W. Information Quarterly for Computer Simulation of Condensed Phases: The CCP5 Newsletter. Vol. 26, p. 43, 1987.

[4] Smith, W. Information Quarterly for Computer Simulation of Condensed Phases: The CCP5 Newsletter. Vol. 39, p. 14, 1993.

NO. OF COPIES	ORGANIZATION
2	DEFENSE TECHNICAL INFO CTR ATTN DTIC DDA 8725 JOHN J KINGMAN RD STE 0944 FT BELVOIR VA 22060-6218
1	HQDA DAMO FDQ ATTN DENNIS SCHMIDT 400 ARMY PENTAGON WASHINGTON DC 20310-0460
1	US MILITARY ACADEMY MATH SCI CTR OF EXCELLENCE DEPT OF MATHEMATICAL SCI ATTN MDN A MAJ DON ENGEN THAYER HALL WEST POINT NY 10996-1786
1	DIRECTOR US ARMY RESEARCH LAB ATTN AMSRL CS AL TP 2800 POWDER MILL RD ADELPHI MD 20783-1145
1	DIRECTOR US ARMY RESEARCH LAB ATTN AMSRL CS AL TA 2800 POWDER MILL RD ADELPHI MD 20783-1145
3	DIRECTOR US ARMY RESEARCH LAB ATTN AMSRL CI LL 2800 POWDER MILL RD ADELPHI MD 20783-1145
	ABERDEEN PROVING GROUND
2	DIR USARL ATTN AMSRL CI LP (305)

NO. OF
COPIES ORGANIZATION

2 UNIV OF PITTSBURGH
DEPT OF CHEMISTRY
ATTN D C SORESCU
D L THOMPSON
PITTSBURGH PA 15260

NO. OF
COPIES ORGANIZATION

ABERDEEN PROVING GROUND

39 DIR, USARL
ATTN: AMSRL-WM-P, A. W. HORST
AMSRL-WM-PC,
B. E. FORCH
G. F. ADAMS
W. R. ANDERSON
R. A. BEYER
S. W. BUNTE
C. F. CHABALOWSKI
K. P. MCNEILL-BOONSTOPPEL
A. COHEN
R. DANIEL
D. DEVYNCK
R. A. FIFER
J. M. HEIMERL
B. E. HOMAN
A. JUHASZ
A. J. KOTLAR
R. KRANZE
E. LANCASTER
W. F. MCBRATNEY
K. L. MCNESBY
M. MCQUAID
N. E. MEAGHER
M. S. MILLER
A. W. MIZIOLEK
J. B. MORRIS
J. E. NEWBERRY
W. V. PAI
R. A. PESCE-RODRIGUEZ
J. RASIMAS
B. M. RICE
P. SAEGAR
R. C. SAUSA
M. A. SCHROEDER
R. SCHWEITZER
L. D. SEGER
J. A. VANDERHOFF
D. VENIZELOS
W. WHREN
H. L. WILLIAMS

REPORT DOCUMENTATION PAGE

Form Approved
OMB No. 0704-0188

1. AGENCY USE ONLY *(Leave blank)*	2. REPORT DATE	3. REPORT TYPE AND DATES COVERED
	May 1997	Final, Jan 96 - Dec 96

4. TITLE AND SUBTITLE
Intermolecular Potential for the Hexahydro-1,3,5-trinitro-1,3,5,-s-triazine (RDX) Crystal: A Crystal-Packing, Monte Carlo, and Molecular Dynamics Study

5. FUNDING NUMBERS
PR: 1L161102AH43

6. AUTHOR(S)
Dan C. Sorescu*, Donald L. Thompson, * and Betsy M. Rice

7. PERFORMING ORGANIZATION NAME(S) AND ADDRESS(ES)
U.S. Army Research Laboratory
ATTN: AMSRL-WM-PC
Aberdeen Proving Ground, MD 21005-5066

8. PERFORMING ORGANIZATION REPORT NUMBER
ARL-TR-1358

9. SPONSORING/MONITORING AGENCY NAMES(S) AND ADDRESS(ES)

10.SPONSORING/MONITORING AGENCY REPORT NUMBER

11. SUPPLEMENTARY NOTES
Mr. Sorescu and Mr. Thompson are with Oklahoma State University, Dept. of Chemistry, Stillwater, OK 74078.
*Current mailing address: University of Pittsburgh, Department of Chemistry, Pittsburgh, PA 15260.

12a. DISTRIBUTION/AVAILABILITY STATEMENT
Approved for public release; distribution is unlimited.

12b. DISTRIBUTION CODE

13. ABSTRACT ***(Maximum 200 words)***

We have developed an intermolecular potential that describes the structure of the α-form of the hexahydro-1,3,5-trinitro,1,3,5-s-triazine (RDX) crystal. The potential is composed of pairwise atom-atom (6-exp) Buckingham interactions and charge-charge interactions. The parameters of the Buckingham repulsion-dispersion terms have been determined through a combination of nonlinear least-squares fitting to observed crystal structures and lattice energies and trial-and-error adjustment. Crystal-packing calculations were performed to determine the equilibrium crystallographic structure and lattice energy of the model. There are no significant differences in the geometrical structures and crystal energies resulting from minimization of the lattice energy with and without symmetry constraints. Further testing of the intermolecular potential has been done by performing symmetry-constrained isothermal-isobaric Monte Carlo simulations. The properties of the crystal (lattice dimensions, molecular orientation, and lattice energy) determined from Monte Carlo simulations at temperatures over the range 4.2–300 K indicate good agreement with experimental data. The intermolecular potential was also subjected to isothermal-isobaric molecular dynamics calculations at ambient pressure for temperatures ranging from 4.2 to 325 K. Crystal structures at 300 K are in outstanding agreement with experiment (within 2% of lattice dimensions, and almost no rotational and translational disorder of the molecules in the unit cell). The space-group symmetry was maintained throughout the simulations. Thermal expansion coefficients were determined for the model, and are in reasonable accord with experiment.

14. SUBJECT TERMS
potential energy surface, RDX, molecular dynamics, Monte Carlo, molecular packing

15. NUMBER OF PAGES
51

16. PRICE CODE

17. SECURITY CLASSIFICATION OF REPORT	18. SECURITY CLASSIFICATION OF THIS PAGE	19. SECURITY CLASSIFICATION OF ABSTRACT	20. LIMITATION OF ABSTRACT
UNCLASSIFIED	UNCLASSIFIED	UNCLASSIFIED	UL

NSN 7540-01-280-5500
Standard Form 298 (Rev. 2-89)
Prescribed by ANSI Std. 239-18 298-102

INTENTIONALLY LEFT BLANK.

USER EVALUATION SHEET/CHANGE OF ADDRESS

This Laboratory undertakes a continuing effort to improve the quality of the reports it publishes. Your comments/answers to the items/questions below will aid us in our efforts.

1. ARL Report Number/Author ARL-TR-1358 (Sorescu) Date of Report May 1997

2. Date Report Received _____

3. Does this report satisfy a need? (Comment on purpose, related project, or other area of interest for which the report will be used.) _____

4. Specifically, how is the report being used? (Information source, design data, procedure, source of ideas, etc.) _____

5. Has the information in this report led to any quantitative savings as far as man-hours or dollars saved, operating costs avoided, or efficiencies achieved, etc? If so, please elaborate. _____

6. General Comments. What do you think should be changed to improve future reports? (Indicate changes to organization, technical content, format, etc.) _____

CURRENT ADDRESS

_____
Organization

_____
Name E-mail Name

_____
Street or P.O. Box No.

_____
City, State, Zip Code

7. If indicating a Change of Address or Address Correction, please provide the Current or Correct address above and the Old or Incorrect address below.

OLD ADDRESS

_____
Organization

_____
Name

_____
Street or P.O. Box No.

_____
City, State, Zip Code

(Remove this sheet, fold as indicated, tape closed, and mail.)
(DO NOT STAPLE)

DEPARTMENT OF THE ARMY

OFFICIAL BUSINESS

NO POSTAGE
NECESSARY
IF MAILED
IN THE
UNITED STATES

BUSINESS REPLY MAIL
FIRST CLASS PERMIT NO 0001,APG,MD

POSTAGE WILL BE PAID BY ADDRESSEE

DIRECTOR
US ARMY RESEARCH LABORATORY
ATTN AMSRL WM PC
ABERDEEN PROVING GROUND MD 21005-5066